

1 **Whole blood transcriptome profiles of trypanotolerant and trypanosusceptible cattle**
2 **highlight a differential modulation of metabolism and immune response during infection**
3 **by *Trypanosoma congolense***

4 **Moana Peylhard ^{1,2}, David Berthier ^{1,2}, Guiguigbaza-Kossigan Dayo ³, Isabelle Chantal ^{1,2},**
5 **Souleymane Sylla ³, Sabine Nidelet ^{4,5}, Emeric Dubois ^{4,5}, Guillaume Martin ^{6,7}, Guilhem**
6 **Sempéré ^{1,2}, Laurence Flori ⁸, Sophie Thévenon ^{1,2}**

7 ¹INTERTRYP, Univ. Montpellier, CIRAD, IRD, Montpellier, France

8 ²CIRAD, UMR INTERTRYP, F-34398 Montpellier, France

9 ³Centre International de Recherche-Développement sur l'Elevage en zone Subhumide (CIRDES), 01 BP 454,
10 Bobo-Dioulasso 01, Burkina Faso

11 ⁴Univ. Montpellier, CNRS, INSERM, Montpellier France

12 ⁵Montpellier GenomiX, France Génomique, Montpellier, France

13 ⁶CIRAD, UMR AGAP Institut, F-34398 Montpellier, France

14 ⁷UMR AGAP Institut, Univ Montpellier, CIRAD, INRAE, Institut Agro, Montpellier, France

15 ⁸SELMET, INRAE, CIRAD, Montpellier Supagro, University of Montpellier, Montpellier, France

16 **Corresponding author:** Sophie Thévenon (sophie.thevenon@cirad.fr <https://orcid.org/0000-0001-6059-584>)

17 Moana Peylhard <https://orcid.org/0000-0001-8574-4567>

18 David Berthier <https://orcid.org/0000-0002-3283-6588>,

19 Guiguigbaza-Kossigan Dayo <https://orcid.org/0000-0001-7926-5834>

20 Isabelle Chantal <https://orcid.org/0000-0002-3429-484X>

21 Souleymane Sylla,

22 Sabine Nidelet,

23 Emeric Dubois, <https://orcid.org/0000-0002-6052-4178>

24 Guillaume Martin <https://orcid.org/0000-0002-1801-7500>

25 Guilhem Sempéré <https://orcid.org/0000-0001-7429-2091>

26 Laurence Flori <https://orcid.org/0000-0002-7529-8521>

27 **Abstract**

28 Animal African trypanosomosis, caused by blood protozoan parasites transmitted mainly by tsetse flies,
29 represents a major constraint for millions of cattle in sub-Saharan Africa. Exposed cattle include
30 trypanosusceptible indicine breeds, severely affected by the disease, and West African taurine breeds
31 called trypanotolerant owing to their ability to control parasite development, survive and grow in enzootic
32 areas. Until now the genetic basis of trypanotolerance remains unclear. Here, to improve knowledge of the
33 biological processes involved in trypanotolerance versus trypanosusceptibility, we identified bovine genes
34 differentially expressed in five West African cattle breeds during an experimental infection by *Trypanosoma*
35 *congolense* and their biological functions. To this end, whole blood genome-wide transcriptome of three
36 trypanotolerant taurine breeds (N'Dama, Lagune and Baoulé), one susceptible zebu (Zebu Fulani) and one
37 African taurine x zebu admixed breed (Borgou) were profiled by RNA sequencing at four time points, one
38 before and three during infection. As expected, infection had a major impact on cattle blood transcriptome
39 regardless of the breed. The functional analysis of differentially expressed genes over time in each breed
40 confirmed an early activation of the innate immune response, followed by an activation of the humoral
41 response and an inhibition of T cell functions at the chronic stage of infection. More importantly, we
42 highlighted overlooked features, such as a strong disturbance in host metabolism and cellular energy
43 production that differentiates trypanotolerant and trypanosusceptible breeds. N'Dama breed showed the
44 earliest regulation of immune response, associated with a strong activation of cellular energy production,
45 also observed in Lagune, and to a lesser extent in Baoulé. Susceptible Zebu Fulani breed differed from other
46 breeds in its metabolic regulation. The differential regulation of cellular energy production in the three
47 trypanotolerant breeds suggests a common mechanism of trypanotolerance. The differential regulation of
48 cellular energy production in the three trypanosusceptible breeds suggests a common mechanism of
trypanosusceptibility.

49 breeds by the strongest modification in lipid metabolism regulation. Overall, this study provides a better
50 understanding of the biological mechanisms at work during infection, especially concerning the interplay
51 between immunity and metabolism that seems differentially regulated depending on the cattle breeds.

52 **Introduction**

53 Animal African Trypanosomosis (AAT) represents a serious impediment to livestock development in
54 endemic areas of Africa (Alsan, 2015). This vector-borne disease is caused by blood extracellular protozoan
55 parasites from the *Trypanosoma* genus (e.g., *Trypanosoma congolense*, *T. vivax* and, to a lesser extent, *T.*
56 *b. brucei*) mainly transmitted by tsetse flies (genus *Glossina*). It affects about 50 million cattle in 38
57 countries in humid and sub-humid zones of Africa by causing high morbidity and mortality (Uilenberg,
58 1998), (Swallow, 2000). The Food and Agriculture Organization of the United Nations estimated its annual
59 cost at \$4.5 billion (Budd, 1999), (Mattioli et al., 2004). Up to now, no vaccine is available and the main
60 prophylactic and curative measures are based on the reduction of transmission rates through vector
61 control (Bouyer et al., 2013), and the use of trypanocides in livestock (Meyer et al., 2016).

62 Interestingly, West African taurine (*Bos taurus taurus*) breeds (AFT), such as long-horn (i.e., N'Dama)
63 and short-horn breeds (e.g., Somba, Baoulé and Lagune) that have lived in West Africa for about 4000 years
64 (Payne & Hodges, 1997), (Hanotte et al., 2002), possess the ability to survive and remain productive in
65 tsetse-infested areas by controlling parasitemia and limiting anemia and body weight loss caused by AAT
66 (Murray et al., 1984), (CIPEA, 1979). AFT are thus called trypanotolerant. In contrast, both zebu (*Bos taurus*
67 *indicus*) cattle, which arrived more recently in Africa (<2000 YBP) (Loftus et al., 1994), (Bradley et al., 1996),
68 (Hanotte et al., 2002), and European taurine, which were recently introduced to increase African cattle
69 productivity (Seck et al., 2010), are susceptible to AAT (Roberts & Gray, 1973), (Amene et al., 1991), (Doko
70 et al., 1997).

71 The trypanotolerant character is therefore a remarkable example of livestock adaptation to a selective
72 pressure caused by a pathogenic agent. However, the molecular or biological mechanisms underlying this
73 trait have puzzled researchers for dozens of years, although some immunological and genetic studies
74 provided some clues. Indeed, the first immunological studies pointed out a better adaptive immune
75 response and an earlier monocyte lineage activation in N'Dama compared to African Boran zebu (Authie
76 et al., 1993), (Taylor et al., 1996), (Sileghem et al., 1993). Nevertheless, according to (Naessens et al., 2003),
77 the hematopoietic system, which participates in anemia reduction, was not involved in the control of
78 parasitemia. Moreover, several genetic studies on trypanotolerant and trypanosusceptible breeds revealed
79 the polygenic architecture of trypanotolerance (Murray et al., 1990), (Trail et al., 1991), (Van der Waaij et
80 al., 2003), (Hanotte et al., 2003). Further transcriptomic studies (O'Gorman et al., 2006), (O'Gorman et al.,
81 2009) showed that N'Dama and Boran Zebu exhibited a roughly similar response to infection by
82 trypanosomes, but subtle differences in response intensity or timing were observed, such as a higher IL6
83 and IL10 expression in Boran Zebu, or an enhanced B cell activation in N'Dama. By integrating genomic and
84 transcriptomic data, (Noyes et al., 2011) proposed TICAM1 and ARHGAP15 as two candidate genes for
85 trypanotolerance. However, these findings have not been confirmed by other studies analyzing gene
86 coding sequences in several breeds (Alvarez et al., 2015), (Alvarez et al., 2016). More experiments were
87 performed in mouse models, in which the possibility to knock out candidate genes allows to accurately
88 assess their contribution to tolerance or pathology (Cnops et al., 2015), (Magez et al., 2006), (Magez et al.,
89 2007), (Onyilagha et al., 2015). Nevertheless, mice are not natural hosts of livestock trypanosomes, and
90 important physiological features that differentiate them from cattle (Taylor & Mertens, 1999), (Morrison
91 et al., 2016) prevent to directly transpose results between the two species.

92 So far, studies, which investigated immunological, genetic and transcriptomic features of cattle
93 trypanotolerance, have mainly focused on two breeds, the trypanotolerant N'Dama cattle (long-horn
94 taurine originating from Fouta-Djallon in Republic of Guinea) and the trypanosusceptible Boran Zebu (an
95 East-African Zebu). Nevertheless, other West-African taurine cattle are classified as trypanotolerant (CIPEA,
96 1979), (Akol et al., 1986), (Rege, 1999) among which we recently confirmed, under experimental
97 conditions, the trypanotolerant status of two West African short-horn breeds, i.e., Lagune and Baoulé
98 breeds, compared to N'Dama and to the trypanosusceptible Zebu Fulani (Berthier et al., 2015). We also
99 underlined the intermediate status of Borgou breed, an admixed breed between African short-horn taurine

100 and African zebu. Biological samples collected during this experiment that allowed a clear characterization
101 of the trypanotolerant status of these overlooked breeds provide the opportunity to finely investigate
102 breed-specific modulation of gene expression during infection.

103 In order to increase knowledge on host-parasite interactions in trypanotolerant and trypanosusceptible
104 cattle breeds during trypanosomosis, we performed a gene expression profiling of blood cells of five cattle
105 breeds infected by *T. congolense* using RNA-seq technology, namely the well-characterized trypanotolerant
106 N'Dama breed, two overlooked trypanotolerant breeds, Baoulé and Lagune, the Borgou crossbred breed,
107 and one trypanosusceptible breed, the Zebu Fulani. In addition, we performed an in-depth functional
108 analysis of the differentially expressed genes. More precisely, we looked for i) breed-specific transcriptomic
109 signatures in blood before infection, ii) main genes and biological functions that responded to infection,
110 whatever the breed, iii) breed-specific transcriptomic profiles during infection, and iv) basal and dynamic
111 transcriptomic profiles that could be associated with trypanotolerance.

112 **Material and Methods**

113 **Animals, experimental infection and sampling**

114 A total of 39 animals from five West African cattle breeds, i.e., three AFT comprising N'Dama (NDA, 8
115 animals), Lagune (LAG, 7 animals), and Baoulé (BAO, 8 animals), Zebu Fulani (ZFU, 8 animals), and Borgou
116 (BOR, 8 animals), were experimentally infected by intravenous inoculation of 10^5 trypanosomes of the *T.*
117 *congolense* savannah IL1180 strain. This experimental infection, conducted at CIRDES (Burkina Faso)
118 according to a protocol approved by the Burkinabe ethical committee (Project no. A002-2013 / CE-CM),
119 was described in details in (Berthier et al., 2015).

120 Cattle blood samples were collected at the jugular vein using Tempus™ Blood RNA Tubes (Applied
121 Biosystems™, USA), which allowed the immediate blocking of mRNA transcription and degradation, at four
122 time points: before infection (named DPI.0, DPI for days post-infection) and during the infection at 20 days
123 post-infection (DPI.20), corresponding roughly to the increase in parasitemia, 30 DPI (DPI.30), around the
124 peak of parasitemia, and 40 DPI (DPI.40), at the time of the entrance in the chronic phase of the disease.
125 They were stored 24 hours at +4°C before treatment.

126 **RNA extraction and RNA-seq libraries preparation**

127 RNAs were extracted from blood samples using the Tempus™ Spin RNA Isolation Kit (Applied
128 Biosystems™, USA) according to the manufacturer's instructions. RNA was finally eluted using 80 µl RNase-
129 free buffer. Total RNA was quantified using a Nanodrop One (Thermo Fisher Scientific, USA) and its quality
130 checked on a Bioanalyzer 2100 using RNA 6000 nano kit (Agilent Technologies, USA). Samples with RNA
131 integrity number ≥ 8.70 were selected.

132 RNA-seq libraries were constructed from 120 RNA samples obtained from six cattle per breed at four
133 time points at the MGX platform in Montpellier (France) using the TruSeq Stranded mRNA Library Prep Kit
134 (Illumina) following the manufacturer's instruction. Briefly, poly-A RNAs were purified using oligo-d(T)
135 magnetic beads from 1 µg of total RNA. The poly-A+ RNAs were fragmented and reverse transcribed using
136 random hexamers, Super Script II (Life Technologies) and Actinomycin D. During the second strand
137 generation step, dUTP substituted dTTP in order to prevent the second strand to be used as a matrix during
138 the final PCR amplification. Double stranded cDNAs were adenylated at their 3' ends before ligation that
139 was performed using Illumina's indexed adapters. Ligated cDNAs were amplified following 15 PCR cycles
140 and PCR products were purified using AMPure XP Beads (Beckman Coulter Genomics). Libraries were
141 validated using a Bioanalyzer on a DNA1000 chip (Agilent) and quantified using the KAPA Library
142 quantification kit (Roche).

143 **Sequencing process**

144 Clustering was performed on a cBot and sequencing on a HiSeq2000 (Illumina). After quantification,
145 the libraries were equimolarly pooled by 12, leading to 10 multiplexes of 12 samples each. Assignment to

146 the multiplexes was done by random blocking on the time point and the breed, in order for each multiplex
147 to contain the four time points (3 samples per time point) and the five breeds. Each pool was denatured,
148 diluted and clustered on three lanes using the Cluster Generation kit v3 (Illumina). Sequencing was
149 performed using SBS kit v3 (Illumina) in single read 50 nt mode. Raw sequencing data were saved as FASTQ
150 files. The quality of the data was assessed using FastQC from the Babraham Institute. Potential
151 contaminants were investigated with the FastQ Screen software (the Babraham Institute).

152 **Reads' alignment to the bovine and trypanosome genomes**

153 Reads were jointly mapped to both reference genomes of bovine (EnsemblDB *Bos taurus* UMD 3.1
154 release 79) and parasite (TritypDB *Trypanosoma congolense* IL3000 release 9) using STAR aligner (STAR
155 2.4.0j, (Dobin et al., 2013)). To this end, mapping was performed in four steps: i) the STAR index was
156 generated from a unique multi-FASTA file obtained by concatenation of the bovine and trypanosome
157 sequence files, ii) reads from all libraries were aligned against the indexed reference sequences in order to
158 identify intron-exon junctions, iii) a new STAR index was generated from the unique multi-FASTA file
159 obtained by concatenation of the bovine and trypanosome sequence files and information of intron-exon
160 junctions, iv) a final step of read mapping was performed on the new STAR index. A maximum of three
161 mismatches were allowed and multi-mapping to up to 20 different positions was permitted according to
162 the following parameters: --alignIntronMin 50 --alignIntronMax 500000 --outFilterMultimapNmax 20 --
163 outFilterMismatchNmax 4 --outSAMunmapped Within. Information on reads location on both reference
164 genomes was contained in final BAM format files.

165 The percentages of reads that mapped uniquely to the bovine or to the trypanosome genome and reads
166 that had multiple matches were checked using Picard tools 1.130 (Broad Institute) and Samtools 1.2 (Li et
167 al., 2009). A large majority of reads was uniquely aligned to the bovine genome (85 to 88% and from 73%
168 to 82% for the samples sharing the index with the PhiX control, see S1 Table). The joint mapping approach
169 was validated by the very low number of reads that mapped to both genomes (bovine and trypanosome),
170 comprised between 17 and 124 (from 0.00004% to 0.0003% of input reads). The percentage of reads
171 uniquely aligned to the trypanosome genome varied greatly between samples, from 3×10^{-6} to 2.31%, with
172 a mean of 0.21% (S1 Table). Before the infection (DPI.0), few hundred reads were aligned on the parasite
173 genome, corresponding to a maximum ratio of 3.8×10^{-5} reads (reads uniquely aligned to the trypanosome
174 genome/number of uniquely aligned reads) (S1 Fig). The very low rate of sequences assigned to the
175 parasite genome before infection was considered as negligible and as a background noise of sequencing
176 technology and mapping algorithm (O'Rawe et al., 2015). During the infection (DPI.20, DPI.30, and DPI.40),
177 the number of reads assigned to the trypanosome genome increased and was closely related to
178 parasitemia (S1 Fig). Two animals (BO5 and Z4) did not show any increase in the ratio of reads uniquely
179 aligned to the trypanosome genome.

180 **Transcript quantification and data normalization**

181 Quantification of gene expression was performed for each library using FeatureCounts (Subread
182 package 1.4.6-p4 (Liao et al., 2014)). Bovine gene annotation was downloaded from Ensembl 79 (sequence
183 UMD 3.1). Reads were assigned at the exon level and counts were summarized at the gene level, using
184 default parameters (-t exon -g gene_id), corresponding to unambiguously assigning uniquely aligned single-
185 end reads and reversely stranded reads (-s 2).

186 Following the advised workflow of the Bioconductor package EdgeR 3.18.3 (Robinson et al., 2010), (R
187 Core Team, 2018), we first removed lowly expressed genes, and kept genes that had more than one count
188 per million in at least two libraries. Out of the 24,616 bovine genes annotated in Ensembl 79, 13,107 genes
189 went through the filter. Normalization of count data was performed using the Trimmed Mean of M-values
190 normalization (Robinson et al., 2010) and dispersion was estimated using a Cox-Reid profile-adjusted
191 likelihood (Chen et al., 2014), using the Bioconductor package EdgeR 3.18.3 under R 3.4.0 environment
192 (Robinson et al., 2010), (R Core Team, 2018).

193 **Exploration of the global structuration of bovine count data and sample selection**

194 A two-dimensional scatterplot was launched on the normalized count data to assess the global
195 structuration of 120 samples (Ritchie et al., 2015). It was completed by a Principal Component Analysis
196 (PCA) performed on the log of normalized count per million using mixOmics_6.3.0 (Le Cao et al., 2016)
197 (with center=TRUE and scale=FALSE). The first factorial plan separated the samples according to sampling
198 time point, except for BO5 and Z4 whose samples clustered together (S2 Fig). This observation and the very
199 low ratio of sequences assigned to the trypanosome genome (S1 Fig) supported the hypothesis that the
200 infection process did not occur in BO5 and Z4, in accordance with the phenotypic analysis that revealed
201 transient parasitemia and no anemia in these animals (Berthier et al., 2015). BO5 and Z4 were thus
202 discarded from subsequent analyses. In addition, a Baoulé (BA3) that was detected positive in parasitemia
203 before the experimental infection, contrary to the others that were negative based on diagnostic tests
204 (Berthier et al., 2015), was also excluded from further analyses. The final data set used for statistical and
205 functional analyses contained 108 RNA-seq libraries, corresponding to 27 animals (6 NDA, 6 LAG, 5 ZFU, 5
206 BOR, and 5 BAO) and four time points per animal.

207 **Differential expression analyses of bovine genes**

208 The differential expression analysis of bovine genes was carried out using the Bioconductor package
209 EdgeR 3.18.3 under R 3.4.0 environment (Robinson et al., 2010), (R Core Team, 2018), which models gene
210 count data according to a negative binomial distribution and moderates the degree of over-dispersion
211 across genes. A generalized linear model (GLM) was fitted for each gene, and tests for determining
212 differential expression were done using a likelihood ratio test (McCarthy et al., 2012). We considered
213 nineteen contrasts to assess differential expressions between two conditions using GLM (Fig 1).

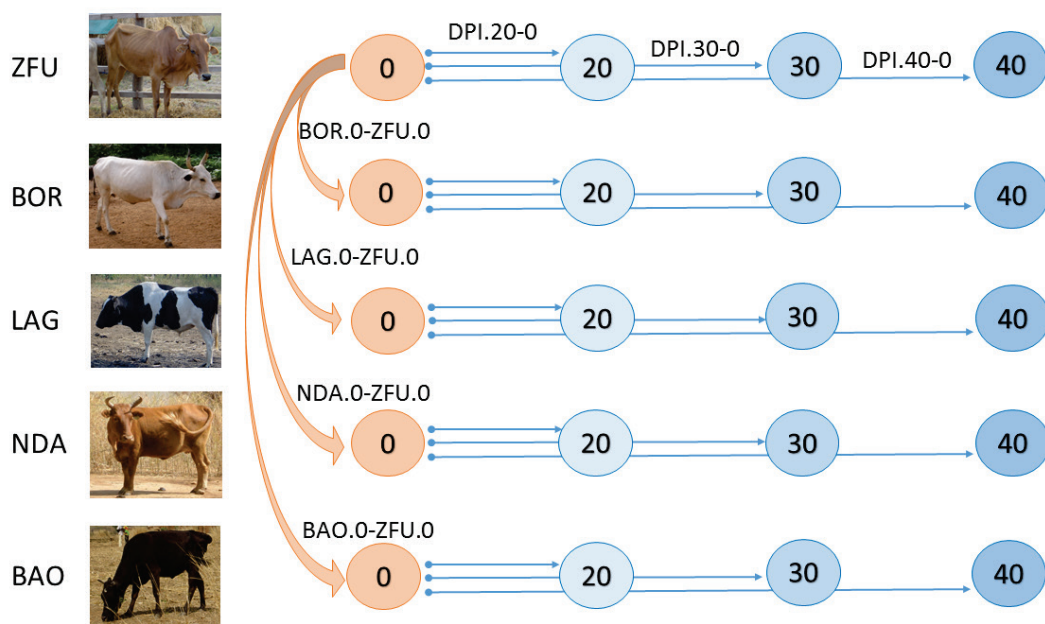


Figure 1. Description of the contrasts used for the differential gene expression analysis. The numbers in the circles represent the days post-infection of cattle sampling, at DPI.0, DPI.20, DPI.30 and DPI.40. Orange arrows represent the contrasts between the breeds at DPI.0, before infection, named BOR.0-ZFU.0, LAG.0-ZFU.0, NDA.0-ZFU.0, and BAO.0-ZFU.0. The blue arrows represent the within-breed contrasts: for each breed, three contrasts were built with DPI.0 as reference, DPI.20-0, DPI.30-0, and DPI.40-0. ZFU, LAG, and BAO pictures by S. Thévenon; BOR picture by G-K. Dayo; NDA picture by D. Berthier.

214 First, to study baseline differential expression between breeds before infection, we chose ZFU as breed
215 reference, the unique indicine trypanosusceptible breed whose samples were placed at the extremity of
216 the second axis in the PCA (S2 Fig). Four contrasts, comparing NDA, LAG, BAO and BOR breeds to ZFU breed
217 at DPI.0 (Fig 1) were established (namely NDA.0-ZFU.0, LAG.0- ZFU.0, BAO.0-ZFU.0 and BOR.0-ZFU.0).
218 Second, to assess how each breed reacted to infection, 15 within breed contrasts, corresponding to three
219 contrasts that assessed differential expression between three post-infection time points and the pre-
220 infection time point (namely DPI.20-0, DPI.30-0 and DPI.40-0, Fig 1), were considered for each breed.
221 Because animals were repeatedly sampled, the design matrix was constructed according to a nested
222 factorial formula, with animals and time points nested within the breed. GLM likelihood ratio tests provided
223 for each contrast and each gene a logFC (log2-fold change of gene expression between conditions) and a
224 FDR (False Discovery Rate) corresponding to adjusted *p*-values for multiple testing using the Benjamini-
225 Hochberg procedure (Benjamini & Hochberg, 1995). In our analyses, since 19 contrasts were done, a FDR
226 of 10^{-3} ($0.05/19=0.0026$ rounded to 0.001) was chosen to identify differentially expressed genes (DEGs).

227 **Functional analysis**

228 The web-based software application Ingenuity® Pathway Analysis (IPA®, Version 43605602, 2018-04-
229 04) was used to perform the functional analysis of the DEGs, based on the content of the Ingenuity®
230 Knowledge Base (IKB).

231 For all contrasts detailed above, among the 13,107 bovine Ensembl identifiers (with their associated
232 logFC and FDR) that defined the background gene list used in IPA® analyses and that were uploaded into
233 the software application, 11,316 identifiers were mapped to their corresponding object in IKB®. We then
234 checked via Ensembl Biomart the existence of human orthologues for the 1,791 bovine identifiers that
235 were not recognized in IKB® and found 577 human orthologues with a high confidence level and a one-to-
236 one match. Human Ensembl identifiers for these 577 genes were then used instead of bovine identifiers in
237 files uploaded into IPA®. At last, 11,893 Ensembl identifiers were mapped to known genes in IKB®.

238 The functional analysis performed with IPA® identified biological diseases and functions, canonical and
239 signaling pathways and upstream regulatory molecules that were significantly enriched in our data sets.
240 Upstream regulators are regulatory molecules that can affect the expression of target DEGs and that may
241 not have been detected as DEG by RNA-seq (because, e.g., they may be expressed in another tissue than
242 the sampled one, or at another time than the sampling date, or because they are endogenous biochemical
243 compounds). Right-tailed Fisher's exact test was used to calculate a *p*-value determining the probability
244 that each biological function and/or disease and canonical pathways assigned to our data sets was due to
245 chance alone. These *p*-values were adjusted using the Benjamini-Hochberg correction method (B-H) for
246 diseases and functions and canonical pathways. Diseases and functions, canonical pathways, and upstream
247 regulators were considered as significant if their corresponding *p*-values were below 10^{-3} (B-H correction),
248 10^{-2} (B-H correction) and 10^{-4} respectively, according to the fact that the quantity of information provided
249 by these functional categories, and thus the number of tests, differed. In addition, based on the logFC of
250 the DEGs and IKB® information, IPA® inferred activation states (namely "activated" or "inhibited") of
251 biological functions, pathways and upstream regulators (indicating that the observed up or down-
252 regulations of the DEGs are mostly consistent with a particular activation state of a biological function or a
253 regulator) by estimating Z-scores associated with the enriched functions or regulators (Kramer et al., 2014).
254 A Z-score ≥ 2 corresponded to an inferred significant activation state of a function or a regulator, while a
255 Z-score ≤ -2 corresponded to an inferred inhibition state. IPA® outputs were visualized using ggplot2 R
256 package (Wickham, 2016).

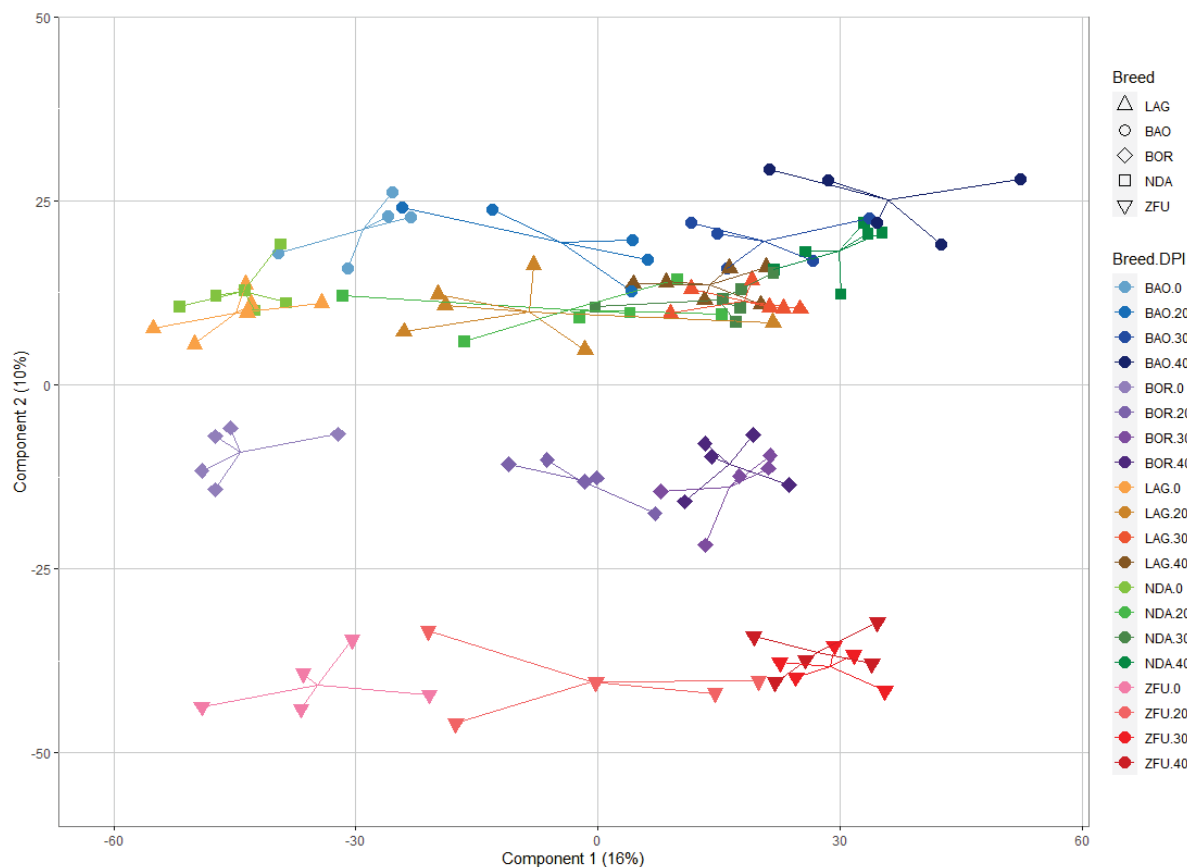
257 **Results**

258 In order to better understand host-parasite interactions in trypanotolerant and trypanosusceptible
259 cattle breeds during infection, we carried out an overall assessment of the relationships between the
260 samples, the identification of initially differentially expressed genes between breeds (i.e., before infection),
261 and the identification of differentially expressed genes in each breed during infection, with a first focus on

262 common DEGs and the core associated biological processes, followed by an enlightenment on biological
263 processes specific or prominent to each breed.

264 **Global overview of bovine gene expression data set**

265 We first carried out an overall assessment of the relationships between the samples, based on a PCA
266 performed on the logarithm of normalized bovine gene counts that provided a global overview of the cattle
267 transcriptomes according to the sampling time point and the breed (Fig 2).



268
269

Figure 2. Principal components analysis of cattle RNA-seq libraries based on normalized genes counts. Each point represents a RNA-seq library that corresponds to an animal sampled at a given DPI and that is plotted on the first two principal components according to its coordinates. Libraries are identified according to the breed and the sampling date. Arrows link a library to the centroid of the corresponding breed and sampling date treatment. Each breed is represented by a different shape and by a color gradient, and each color is graded from light to dark shades corresponding to days post-infection respectively DPI.0, 20, 30 and 40. ZFU animals are in red and triangle down, BOR animals are in violet and diamond, LAG animals are in orange and triangle, BAO animals are in blue and circle, and NDA animals are in green and square. Percentages of variance explanation of the first two components are added.

270 The first axis that accounted for 16% of the total variation was representative of the infection course,
271 from DPI.0 to DPI.40. Shifts from DPI.0 to DPI.40 for each breed were roughly parallel. The second axis that
272 accounted for 10% of the total variation was representative of the breed effect with ZFU count data, at the
273 bottom, taurine count data (represented by NDA, BAO and LAG breeds) at the top and admixed BOR breed
274 data, in the middle, suggesting that basal and lasting count differences existed between zebu, taurine and
275 admixed breeds.

276 Before infection, a total of 310 genes were detected as differentially expressed (DE) between at least
277 one breed and ZFU (FDR<10⁻³). During infection, a total of 5,270 differentially expressed genes (DEGs) were
278 identified in at least one contrast, between 41 and 3,839 genes being DE depending on the contrast (Fig 3).
279

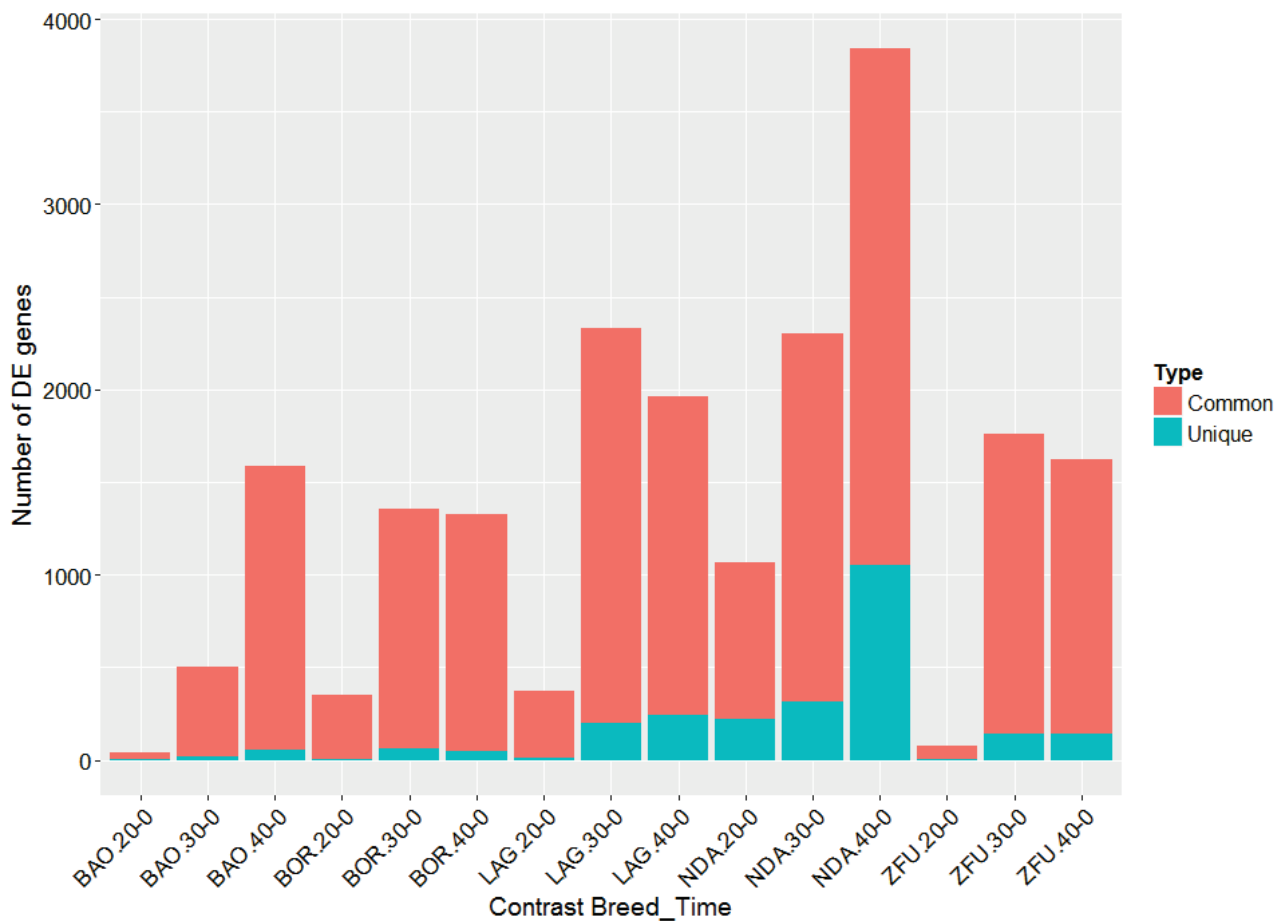
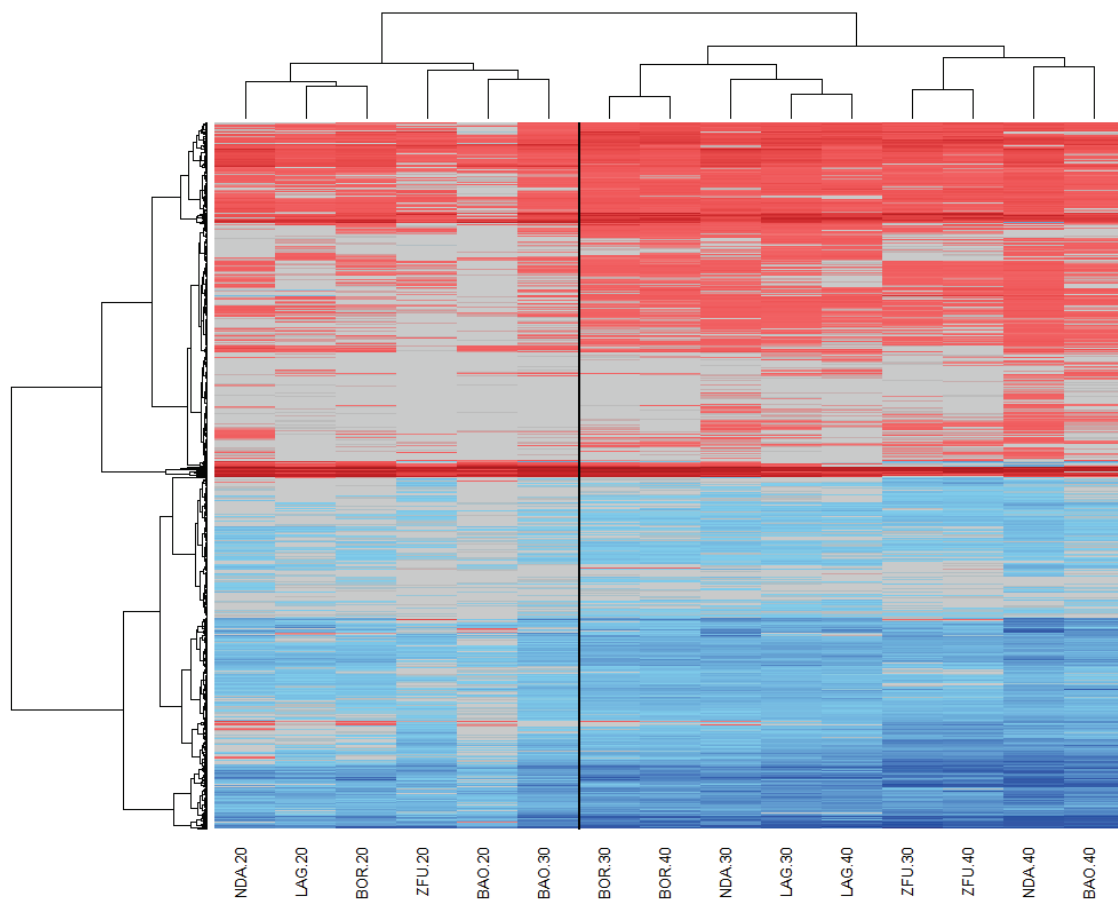


Figure 3. Numbers of genes identified as differentially expressed in the 15 within-breed contrasts. The x-axis represents the 15 contrasts ordered by breed respectively BAO, BOR, LAG, NDA and ZFU, and for each breed, three contrasts according to days post-infection in comparison with before infection, respectively DPI.20-0, 30-0, 40-0. The y-axis represents the number of differentially expressed genes at the threshold of FDR<0.001. The red color corresponds to the part of genes that are differentially expressed and common to, at least, two breeds whatever the sampling time point; the blue color corresponds to the part of genes that are differentially expressed uniquely within a breed.

280 As expected, the bovine transcriptome was massively modified by trypanosome infection, the total
281 number of DEGs during infection being in descending order 4,344, 2,715, 2,141, 1,753 and 1,696 for NDA,
282 LAG, ZFU, BOR and BAO, respectively. NDA displayed the earliest modulation of its transcriptome, with
283 1,067 DEGs at DPI.20-0, followed by LAG (370 DEGs), BOR (351 DEGs), ZFU (77 DEGs), and BAO (41 DEGs)
284 (Fig 3). At DPI.30-0, LAG displayed the highest number of DEGs (2,330). At DPI.40-0, NDA showed again the
285 highest number of DEGs (3,839). Many DEGs were common between two or more breeds including the
286 trypanosusceptible ZFU (Fig 3 and S3 Fig). A total of 3,283 genes (62.3% of total number of DEGs, so a
287 majority) were shared between at least two breeds. For instance, 1,823 DEGs were shared between NDA
288 and ZFU, 1,318 between LAG and ZFU, 1,074 between BOR and ZFU, and 1,069 between BAO and ZFU (S3
289 Fig), whereas the number of DEGs detected exclusively within a breed was 1,272 in NDA, 331 in LAG, 211
290 in ZFU, 96 in BOR and 77 in BAO. Interestingly, the direction of variation of DEGs, when detected DE in
291 several contrasts, whatever the time point or the breed, was always identical in the aforementioned
292 contrasts (i.e., upregulated with positive logFC or downregulated with negative logFC) except for one gene,

293 SPARC, which was upregulated in LAG.40-0 but downregulated in BAO.40-0 (S2 Table). The heatmap (Fig
294 4), performed on the logFCs of 5,270 DEGs in at least one contrast, first clustered contrasts according to
295 the time of infection, the early date (DPI.20-0) being separated from the others, except for the contrast
296 BAO.30-0. At later time points, contrasts from a same breed tended to cluster together (LAG.30-0 with
297 LAG.40-0, BOR.30-0 with BOR.40-0, ZFU.30-0 with ZFU.40-0), although NDA.40-0 and BAO.40-0 were not
298 close to NDA.30-0 and BAO.30-0 respectively. Fig 4 did not highlight obvious different patterns of gene
299 expression between breeds.



300 .

Figure 4. Heatmap on the logFC of 5,270 DEGs in the 15 within-breed contrasts. Columns represent the within-breed contrasts ordered according to clustering, and rows the genes identified as DE in at least one contrast. Up-regulated genes (i.e. with positive logFC) are colored in warm colors from light red to dark red (estimated maximum logFC=11.3), whereas down-regulated genes (i.e. with negative logFC) are colored in cold colors, from light blue to dark blue (estimated minimum logFC=-8.00). LogFC comprised between -0.20 and 0.20 are colored in grey.

301 **Transcriptome profiling before infection highlights basal differences between breeds.**

302 We then focused on the differences before infection of gene expression levels between each breed and
303 ZFU taken as trypanosusceptible reference. For the contrasts LAG.0-ZFU.0, NDA.0-ZFU.0, BAO.0-ZFU.0 and
304 BOR.0-ZFU.0 respectively, 127, 152, 156, and 63 genes were differentially expressed at the FDR threshold
305 of 10^{-3} (Table S3), showing initial differences between gene counts in ZFU and in the other taurine or
306 admixed breeds. As expected from PCA results, the number of DEGs between ZFU and BOR was smaller
307 than those between ZFU and AFT (i.e., NDA, BAO, LAG) at DPI.0. The functional annotation of DEGs for the
308 four contrasts before infection using IPA® indicated that basal differences were not associated with specific

309 biological function enrichment, since neither any disease and function nor any canonical pathway was
310 significantly enriched in these gene sets. However, fifteen upstream regulators, precisely 1, 1, and 15 for
311 the contrasts LAG.0-ZFU.0, BAO.0-ZFU.0 and BOR.0-ZFU.0 respectively, were identified at a p -value $<10^{-4}$
312 (S4 Table). Not any upstream regulator was significantly enriched in NDA.0-ZFU.0. Only BSG, encoding a
313 plasma membrane protein involved in several molecular functions (i.e., cadherin binding, carbohydrate
314 binding, mannose binding, monocarboxylic acid transmembrane transporter activity, and protein binding)
315 was identified as upstream regulator in the three contrasts involving LAG, BAO and BOR. Several upstream
316 regulators linked to immune response (e.g., IL4, TNF, IFNG, Immunoglobulin, CD3 complex, prostaglandin
317 E2, IL10RA) and transcription regulators (e.g., HDAC3, FOXA2, STAT3, ATF3) were enriched in the BOR.0-
318 ZFU.0 gene set.

319 Among the DEGs before infection, 35, 54, 83 and 18 genes were only DE in LAG.0-ZFU.0, NDA.0-ZFU.0,
320 BAO.0-ZFU.0 and BOR.0-ZFU.0 contrasts, respectively (S4 Fig). Besides, twelve genes were found DE in the
321 four contrasts, 36 were shared between the three AFT breeds versus ZFU.0, and 70 were shared between
322 LAG.0-ZFU.0 and NDA.0-ZFU.0. Among these latter 70 DEGs, all genes except PELI3 were downregulated in
323 LAG and NDA in comparison to ZFU, among which several genes are known to be linked to immune
324 response, especially IL2RA, GBP2, PELI3, DCSTAMP, PTX3, and MARCO (S3 Table).

325 **Transcriptomic responses common to all breeds, involving immune response and metabolism, are**
326 **detected during infection**

327 *Genes differentially expressed during infection in all breeds.*

328 To understand the core response of bovine transcriptome to trypanosome infection, we studied the
329 659 DEGs common to all breeds (namely DEGs in at least one contrast of each breed, S3 Fig). S2 Table gives
330 detailed information on each gene by indicating whether it was DE, in which breed, and its average FDR
331 and logFC. Six genes (NR4A1, CCL22, IFI30, CTSZ, KYNU, IL17REL), involved in immune response, were
332 significantly upregulated in all contrasts, meaning that they were DE within each breed at each time point
333 during infection (S2 Table). Among the top upregulated genes (i.e., harboring the highest average logFC),
334 we found HBM, coding for a hemoglobin subunit (average logFC=6.96, average $-\log_{10}(FDR)=5.7$), ARG1
335 (average logFC=6.90, average $-\log_{10}(FDR)=6.0$), and several genes involved in immune response like
336 MAPK12, MMP14 and MAPK11. The top downregulated genes (i.e., DEGs displaying the smallest negative
337 logFC) were UNC5A (average logFC =-2.84, average $-\log_{10}(FDR)=4.7$) followed by OVOS2, ELANE, DAB2,
338 and BPI. A quick overview of potentially interesting DEGs associated with immune response allowed
339 highlighting three cytokines (i.e., IL7 upregulated; IL16 and LIF downregulated) and cytokine receptors (e.g.,
340 IL1R, IL6R, IL7R, IL20RB, all down-regulated), transcription regulators (e.g., NFKB1 and NFKB2 upregulated),
341 other receptors (e.g., TFRC upregulated), and numerous immune cell antigens, some up-regulated (e.g.,
342 CD109, CD180, CD19, CD1A, CD22, CD40, CD72, CD79B, and MME syn.CD10), and others down-regulated
343 (e.g., CD7, CD2, CD226, CD247, CD27, CD3D, CD3E, CD3G, CD40LG, CD99, and ZAP70). Interestingly, several
344 genes known to be involved in metabolism were up-regulated (e.g., HMGCS1, CYP51A1, FDFT1, IDI1, LSS,
345 MVD, SQLE).

346 *Enrichment of diseases and functions in the common DEGs.*

347 The functional annotation of DEGs common to the breeds using IPA® identified 164 functions and
348 diseases significantly enriched with B-H corrected p -values $<10^{-3}$ (S5 Table), and they could be grouped into
349 24 large categories displayed in Table 1. The major categories were cell-to-cell signaling and interaction,
350 cellular movement, cellular development, cell death and survival, hematological system development and
351 function, cellular function and maintenance, and lipid metabolism. We could also highlight cell-mediated
352 immune response, immunological disease, inflammatory response, and lymphoid tissue structure and
353 development. More precisely, the top ten diseases and functions in terms of B-H corrected p -values ($<10^{-8}$)
354 were: proliferation of lymphocytes, proliferation of lymphatic system cells, proliferation of blood cells,
355 proliferation of immune cells, lymphopoiesis, synthesis of sterol, synthesis of cholesterol, quantity of
356 leukocytes, quantity of lymphocytes, and cell movement of lymphatic system cell (S5 Table). IPA® analyses

357 allowed us to assess the activation or inhibition of the enriched diseases and functions based on the Z-
358 score, considered significant if its absolute value was larger or equal to 2. Twenty-four diseases and
359 functions presented significant Z-scores, and surprisingly most had negative Z-scores that could be related
360 to an inhibition state, for instance: lymphocyte homeostasis, adhesion of lymphocytes, migration of
361 lymphatic system cell, and T cell development. Only two diseases and functions had positive Z-score,
362 namely quantity of B-2 lymphocytes and liver lesion.
363

Table 1. Diseases and functions categories enriched in the common DEGs in the within-breed
contrasts. The name of diseases and functions categories was indicated, with for each category, the
number of significant functions, their average B-H corrected *p*-value, the range of the B-H corrected
p-values, the average Z-score, and its range. Na: not available.

364

| Diseases and functions category | Number of functions | Average B-H <i>p</i> -value | Range of B-H <i>p</i> -values | Average Z-score | Range of Z-scores |
|---|---------------------|-----------------------------|--|-----------------|-------------------|
| Cell-To-Cell Signaling and Interaction | 28 | 5.7E-05 | 7x10 ⁻⁴ ; 10 ⁻⁸ | -1.78 | -2.71 ; 1.13 |
| Cellular Movement | 19 | 1.5E-04 | 9x10 ⁻⁴ ; 5x10 ⁻⁹ | -1.45 | -2.66 ; 0.54 |
| Cellular Development | 18 | 1.0E-04 | 7x10 ⁻⁴ ; 3x10 ⁻¹² | -0.34 | -2.08 ; 1.02 |
| Cell Death and Survival | 16 | 1.5E-04 | 9x10 ⁻⁴ ; 6x10 ⁻⁷ | -1.09 | -2.36 ; 0.03 |
| Hematological System Development and Function | 15 | 2.5E-04 | 9x10 ⁻⁴ ; 4x10 ⁻⁹ | -0.54 | -2.07 ; 2.25 |
| Cellular Function and Maintenance | 9 | 2.4E-04 | 9x10 ⁻⁴ ; 2x10 ⁻⁷ | -0.87 | -2.82 ; 0.14 |
| Lipid Metabolism | 8 | 1.1E-05 | 6x10 ⁻⁵ ; 6x10 ⁻¹⁰ | 1.10 | 0.70 ; 1.63 |
| Cancer | 6 | 2.1E-04 | 6x10 ⁻⁴ ; 5x10 ⁻⁶ | -0.05 | -0.43 ; 0.33 |
| Cell Morphology | 6 | 1.9E-04 | 97x10 ⁻⁴ ; 3x10 ⁻⁵ | -0.73 | -1.00 ; -0.47 |
| Cell-mediated Immune Response | 6 | 1.7E-04 | 5x10 ⁻⁴ ; 6x10 ⁻⁸ | -2.11 | -2.65 ; -1.77 |
| Cell Signaling | 5 | 3.5E-04 | 9x10 ⁻⁴ ; 5x10 ⁻⁶ | -0.38 | -1.04 ; -0.05 |
| Immunological Disease | 5 | 2.0E-04 | 7x10 ⁻⁴ ; 3x10 ⁻⁶ | -1.52 | -2.35 ; -0.67 |
| Inflammatory Response | 5 | 1.5E-04 | 7x10 ⁻⁴ ; 5x10 ⁻⁸ | -0.72 | -2.39 ; 1.21 |
| Lymphoid Tissue Structure and Development | 4 | 2.3E-04 | 9x10 ⁻⁴ ; 5x10 ⁻⁸ | -0.43 | -1.15 ; 0.11 |
| Connective Tissue Disorders | 2 | 2.2E-05 | 3x10 ⁻⁵ ; 9x10 ⁻⁶ | 0.05 | -0.13 ; 0.23 |
| Embryonic Development | 2 | 5.4E-04 | 9x10 ⁻⁴ ; 2x10 ⁻⁴ | -0.58 | -1.14 ; -0.02 |
| Inflammatory Disease | 2 | 7.0E-05 | 8x10 ⁻⁵ ; 5x10 ⁻⁵ | -0.76 | -2.43 ; 0.90 |
| Organismal Development | 2 | 1.1E-04 | 2x10 ⁻⁴ ; 2x10 ⁻⁵ | Na | Na |
| Cellular Growth and Proliferation | 1 | 3.3E-12 | | -0.21 | |
| Tissue Morphology | 1 | 2.6E-06 | | -0.16 | |
| Molecular Transport | 1 | 3.2E-04 | | -0.76 | |
| Gastrointestinal Disease | 1 | 5.3E-04 | | 2.06 | |
| Cardiovascular Disease | 1 | 9.6E-04 | | Na | |
| Connective Tissue Development and Function | 1 | 9.6E-04 | | 0.60 | |

365 *Enrichment of canonical Pathways in the common DEGs.*

366 Twenty-three canonical pathways were significantly enriched in common DEGs with a B-H corrected *p*-
367 value $<10^{-2}$ (Table 2). This list highlighted several enriched and activated metabolic pathways (Z-score ≥ 2),
368 e.g., the superpathway of cholesterol biosynthesis, the mevalonate pathway, the TCA (TriCarboxylic acid)
369 cycle II, and the superpathway of geranylgeranyldiphosphate biosynthesis I. Mitochondrial dysfunction was
370 also enriched but without inference on the direction of activation. The second class of enriched pathways
371 concerned the immune response including, for instance, role of NFAT in regulation of the immune
372 response, primary immunodeficiency signaling, and regulation of IL-2 expression in activated and anergic
373 T lymphocytes. Two immune response pathways, PI3K signaling in B lymphocytes and B cell receptor
374 signaling, were estimated as significantly activated.

Table 2. Canonical and signaling pathways enriched in the common DEGs in the within-breed
contrasts. The name of the canonical and signaling pathways is indicated with its B-H corrected *p*-value,
its Z-score, and the ratio between the number of DEGs and the number of genes in the pathway.
Highlighted cells correspond to Z-scores with an inferred activation state.

| Canonical and signalling pathways | B-H <i>p</i> -value | Z-score | Ratio |
|---|---------------------|---------|-------|
| Superpathway of Cholesterol Biosynthesis | 5.2E-08 | 3.61 | 0.52 |
| Mevalonate Pathway I | 6.9E-04 | 2.45 | 0.60 |
| TCA Cycle II (Eukaryotic) | 6.9E-04 | 2.83 | 0.40 |
| Superpathway of Geranylgeranyldiphosphate Biosynthesis I (via Mevalonate) | 6.9E-04 | 2.65 | 0.50 |
| Mitochondrial Dysfunction | 1.7E-03 | Na | 0.15 |
| Role of NFAT in Regulation of the Immune Response | 1.7E-03 | 0.22 | 0.15 |
| Primary Immunodeficiency Signaling | 1.7E-03 | Na | 0.32 |
| PI3K Signaling in B Lymphocytes | 1.7E-03 | 2.32 | 0.16 |
| Cholesterol Biosynthesis I | 1.7E-03 | 2.45 | 0.46 |
| Cholesterol Biosynthesis II (via 24,25-dihydrolanosterol) | 1.7E-03 | 2.45 | 0.46 |
| Cholesterol Biosynthesis III (via Desmosterol) | 1.7E-03 | 2.45 | 0.46 |
| Regulation of IL-2 Expression in Activated and Anergic T Lymphocytes | 2.4E-03 | Na | 0.18 |
| Leukocyte Extravasation Signaling | 4.5E-03 | 0.73 | 0.14 |
| Hematopoiesis from Pluripotent Stem Cells | 4.8E-03 | Na | 0.38 |
| T Cell Receptor Signaling | 5.1E-03 | Na | 0.16 |
| Sirtuin Signaling Pathway | 5.2E-03 | -0.78 | 0.12 |
| IL-7 Signaling Pathway | 5.5E-03 | 0.30 | 0.19 |
| iCOS-iCOSL Signaling in T Helper Cells | 5.6E-03 | 0.33 | 0.17 |
| CD28 Signaling in T Helper Cells | 7.1E-03 | -0.30 | 0.15 |
| B Cell Development | 7.1E-03 | Na | 0.33 |
| Systemic Lupus Erythematosus In B Cell Signaling Pathway | 7.1E-03 | -0.21 | 0.12 |
| B Cell Receptor Signaling | 7.1E-03 | 2.68 | 0.13 |
| Phospholipase C Signaling | 8.9E-03 | 0.24 | 0.12 |

375

376 *Enrichment of upstream Regulators in the common DEGs.*

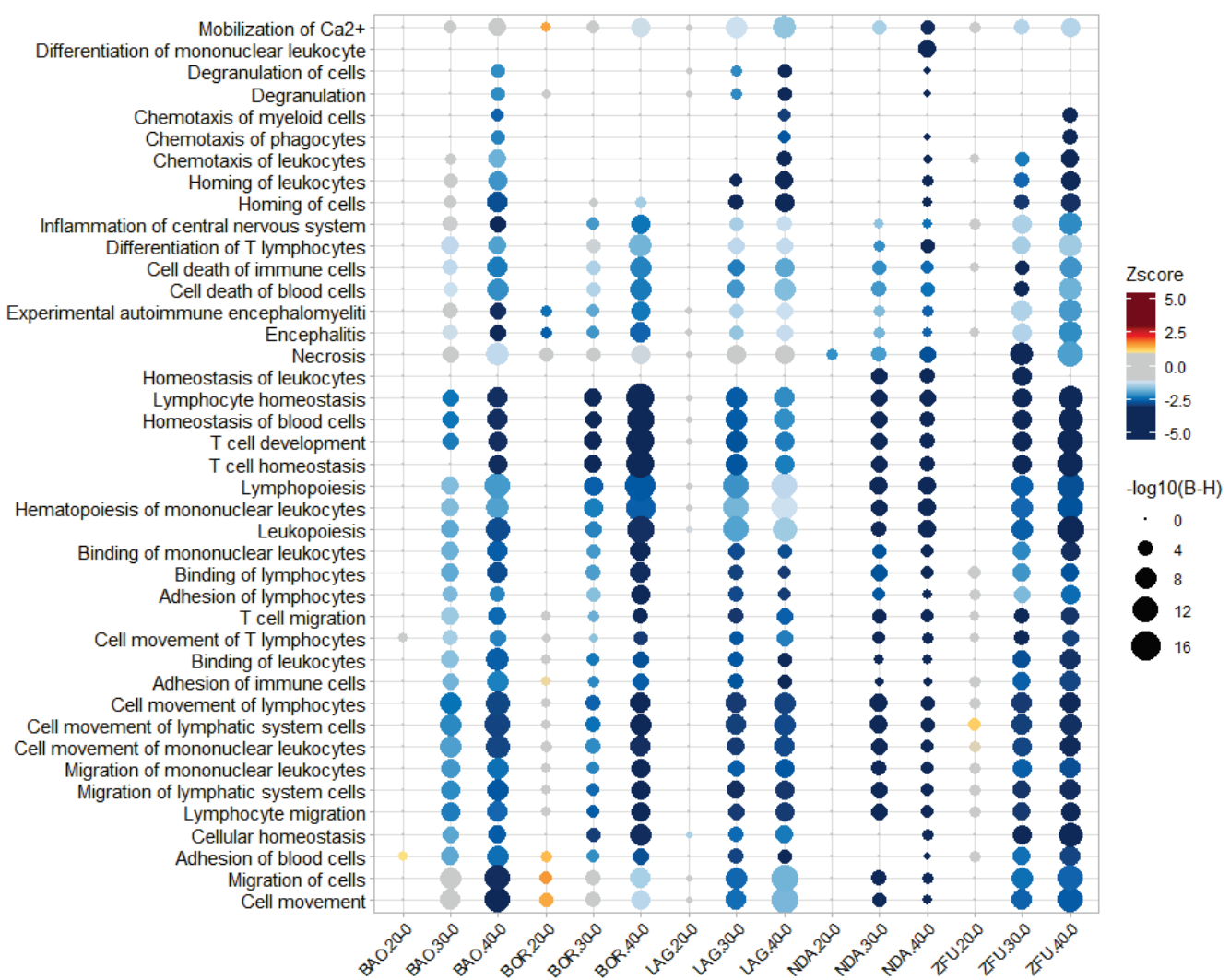
377 Seventy-three upstream regulators that can affect the expression of target DEGs were considered as
378 significantly enriched (P -value $<10^{-4}$, S6 Table), and the direction of activation was inferred for some of
379 them. The list of upstream regulators referred to chemicals, simple protein or protein complexes. Four
380 endogenous chemicals were identified: cholesterol, which was inferred as inhibited, beta-estradiol,
381 prostaglandin E2 and D-glucose. Nine cytokines were significantly enriched: TNF, IL15, IL4, IL3, IFNG, IL10,
382 CSF1, the latter being estimated as activated, and IL2 and IL7, both estimated as inhibited. Detected protein
383 complexes were also related to immune response (i.e., immunoglobulin, C4BP, TCR, IgE, and NFkB).
384 Twenty-seven transcription regulators were identified, some involved in metabolism (e.g., the activated
385 SREBF2, SREBF1, and PPARGC1B), cell cycle (e.g., TP53 inhibited, SP1) or in pleiotropic functions (e.g., SIRT2
386 activated). Several transcription factors were linked to immune response (e.g., STAT6 and STAT3, TCF3
387 inhibited, and BCL6 activated).

388 **Specific transcriptomic response of each breed during infection**

389 In order to look for potential breed-specific responses during infection, we performed separate
390 enrichment analyses of the lists of DEGs of the 15 within-breed contrasts.

391 *Enrichment of diseases and functions in each breed during infection.*

392 The analysis identified 642 diseases and functions significantly enriched in at least one of the 15
393 contrasts (B-H corrected p -values $<10^{-3}$) (S7 Table). The most enriched contrast was ZFU.40-0 with 365
394 significant diseases and functions, while no disease and function were enriched in LAG.20-0. As for the
395 enrichment of the common DEGs, large categories were cellular development and cell cycle, hematological
396 system development and function, immune response, cell signaling, and lipid metabolism. Among these
397 642 diseases and functions, 135 displayed significant Z-scores for the corresponding contrasts, 17 being
398 considered as activated (Z-score ≥ 2), while a majority (118) was inhibited (Z-score ≤ -2). We confirmed the
399 results obtained with the analysis of common DEGs, namely a shared inhibition of numerous cellular
400 functions, especially associated with cell-mediated immune response from 30 DPI (e.g., T cell homeostasis).
401 Fig 5 represents both the significance level and the inhibition state of 41 diseases and functions harboring
402 Z-scores smaller than -3 for the 15 contrasts. Few inhibited functions were set up exclusively by one or few
403 breeds such as the differentiation of mononuclear leukocytes, significantly inhibited in NDA.40-0 only.
404 Chemotaxis of myeloid cells was inhibited in BAO.40-0, LAG.40-0, and ZFU.40-0 contrasts but was
405 considered significantly enriched in ZFU only.



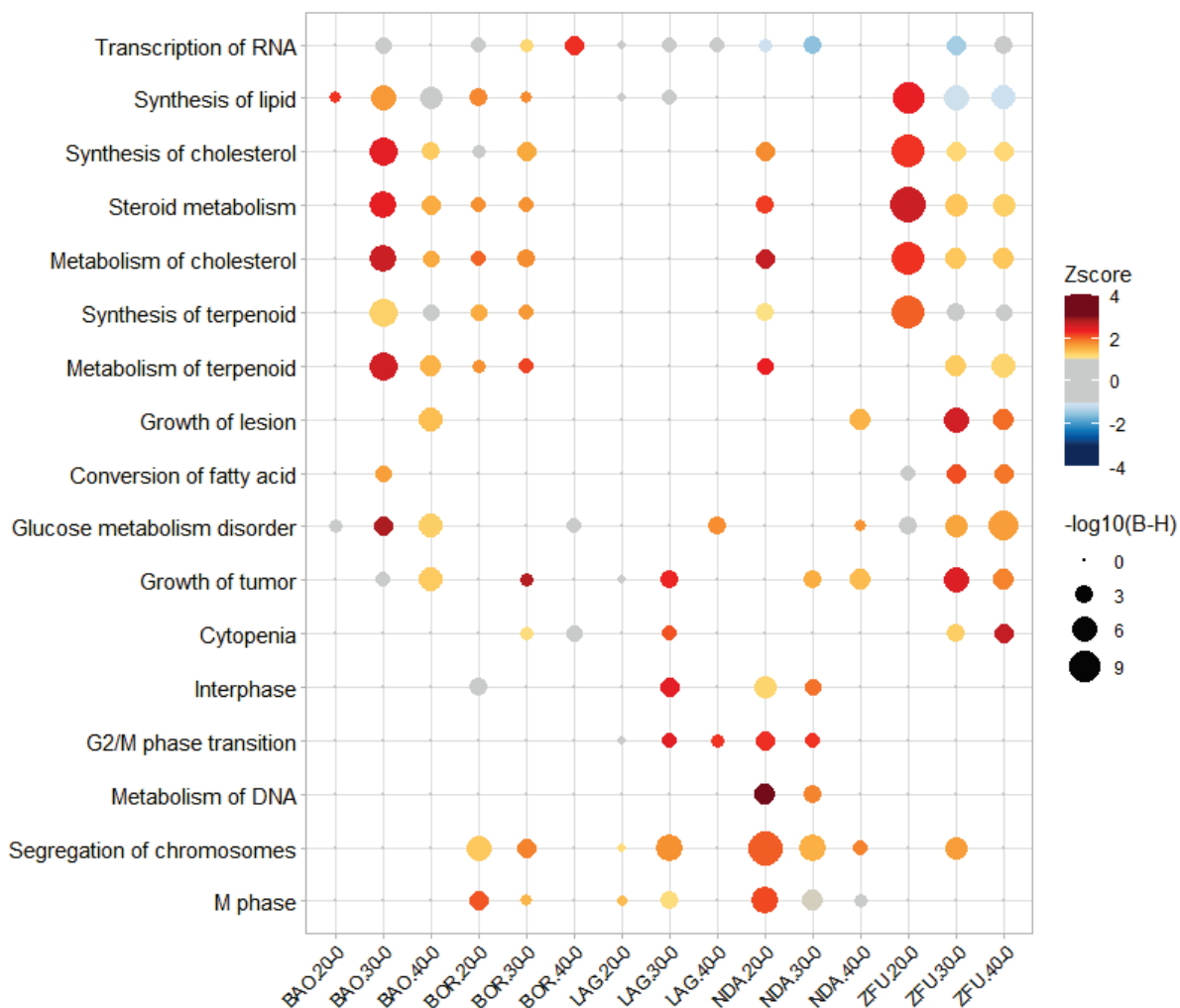
406

Figure 5. Plot of 41 significantly enriched diseases and functions inferred as inhibited in function of the within-breed contrasts. The 15 within-breed contrasts are shown on the abscissa and the significantly enriched diseases and functions on the ordinate. The size of the circles is inversely proportional to the B-H corrected *p*-value calculated for diseases and functions in the aforementioned contrast. The color gradient of the circle corresponds to the Z-score range, i.e. warm color gradient for positive Z-score > 1, cold color gradient for negative Z-score < -1, and gray color gradient for Z-scores ranging between -1 and 1.

407 Fewer diseases and functions were activated, but they presented more discriminating patterns than
408 inhibited functions. Fig 6 shows that lipid metabolic functions (synthesis of lipid, synthesis of cholesterol,
409 steroid metabolism, metabolism of cholesterol, and synthesis of terpenoid) were strongly enriched and
410 activated in ZFU.20-0 contrast, to a lesser extent in BAO.30-0, and slightly in NDA.20-0, but were not
411 detected in LAG. Glucose metabolism disorder was enriched in ZFU and BAO, but activated in BAO.30-0
412 contrast only. Cytopenia was significantly activated in ZFU.40-0 contrast.

413 The cancer category (i.e., 63 significant functions) and cell cycle functions (i.e., 19 significant functions
414 like cell cycle progression, mitosis) were especially and precociously enriched in NDA.20-0 (S7 Table). G2/M
415 phase transition, metabolism of DNA, segregation of chromosomes, and M phase were strongly activated

416 in NDA.20-0 contrast. This latter was also found activated in BOR.20-0. Interphase was activated in LAG.30-
417 0. BOR.40-0 presented an activation of RNA transcription.
418



419

Figure 6. Plot of 17 significantly enriched diseases and functions inferred as activated in function of the within-breed contrasts. The 15 within-breed contrasts are shown on the abscissa and the significantly enriched diseases and functions on the ordinate. The size of the circles is inversely proportional to the B-H corrected p -value of the diseases and functions in the aforementioned contrast. The color gradient of the circle corresponds to the Z-score range, i.e. warm color gradient for positive Z-score >1 , cold color gradient for negative Z-score <-1 , and gray color gradient for Z-scores ranging between -1 and 1.

420 *Enrichment of canonical pathways in each breed during infection.*

421 A total of 92 canonical pathways were significantly enriched in at least one contrast during infection,
422 with a B-H corrected p -value $<10^{-2}$ (S8 Table). The contrast ZFU.40-0 displayed the highest number of
423 significant canonical pathways (48), followed by BAO.30-0 (39), while no significant pathways were
424 detected in LAG.20-0, LAG.40-0, and BAO.20-0. Among the 92 significant canonical pathways, 26 presented
425 also significant Z-scores, measuring their activation state: 7 being considered inhibited and 19 activated
426 (Fig 7).

427

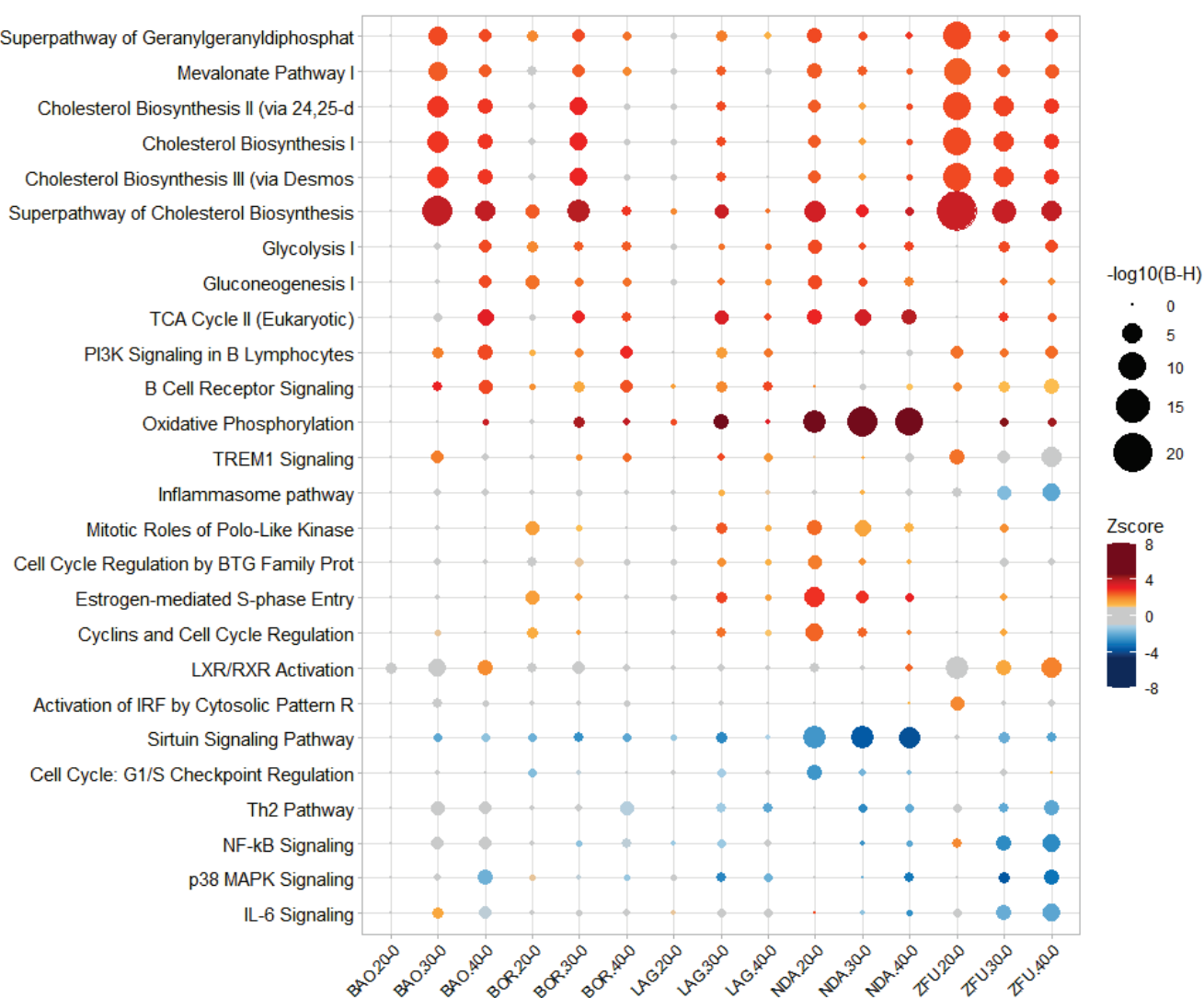


Figure 7. Plot of 26 significantly enriched canonical pathways inferred as activated or inhibited in function of the within-breed contrasts. The 15 within-breed contrasts are shown on the abscissa and the significantly enriched diseases and functions on the ordinate. The size of the circles is inversely proportional to the B-H corrected p -value of the canonical pathways in the aforementioned contrast. The color gradient of the circle corresponds to the Z-score range, i.e. warm color gradient for positive Z-score > 1 , cold color gradient for negative Z-score < -1 , and gray color gradient for Z-scores ranging between -1 and 1.

428 The superpathway of cholesterol biosynthesis was found significantly activated in all breeds, at one
 429 (LAG and NDA), two (BAO and BOR) or three time points (ZFU), but the set of pathways related to
 430 cholesterol and lipid metabolism was particularly and durably enriched in ZFU, and to a lesser extent in
 431 BAO. Likewise, LXR/RXR was activated in ZFU.40-0 and almost in BAO.40-0.

432 Conversely, oxidative phosphorylation, TCA cycle, mitochondrial dysfunction, sirtuin signaling pathway
 433 and cell cycle associated pathways were highly significant in NDA contrasts. Pathways associated with cell
 434 energy production, oxidative phosphorylation and TCA cycle, were strongly activated in NDA, and to a
 435 lesser extent in LAG (oxidative phosphorylation and TCA cycle) and BAO (TCA cycle). Glycolysis and
 436 gluconeogenesis were considered enriched and activated in NDA.20-0, and gluconeogenesis was also
 437 significantly activated in BOR.20-0. Cell cycle associated pathways (Estrogen-mediated S-phase Entry,
 438 Cyclins and Cell Cycle Regulation, Cell Cycle Regulation by BTG Family Proteins, and mitotic Roles of Polo-

439 Like Kinase) were activated in NDA.20-0 exclusively. The sirtuin signaling pathway was highly inhibited in
440 NDA during the infection, and the G1/S checkpoint regulation was inhibited in NDA.20-0.

441 Some pathways, linked to immune response, were transiently enriched in some breeds, but not in NDA,
442 and their direction of activation was not able to be inferred (i.e., leukocyte extravasation signaling
443 significant in ZFU.40-0, LAG.30-0, and BAO.30-0 and BAO.40-0; hematopoiesis from pluripotent stem cells
444 significant in LAG.30-0, BAO.30-0 and BAO.40-0, and BOR.40-0; natural killer signaling significant in ZFU,
445 BAO and BOR at 40-0). Two B-cell associated pathways (B Cell Receptor signaling, and PI3K Signaling in B
446 Lymphocytes) were activated in BAO.40-0. Interestingly, five pathways were significantly inhibited in
447 ZFU.30-0 and/or ZFU.40-0 (i.e., IL-6 Signaling, NF- κ B Signaling, p38 MAPK Signaling, Th2 pathway and the
448 inflamasome pathway).

449 *Upstream Regulators enriched in each breed during infection.*

450 316 upstream regulators that can affect the expression of target DEGs were considered as significantly
451 enriched in at least one contrast (P -value $<10^{-4}$, S9 Table). Among them, 95 upstream regulators belonged
452 to the transcription regulator category, 29 were endogenous chemicals and 26 were cytokines according
453 to IPA® classification. Upstream regulators found significant in almost all contrasts at the chosen threshold
454 were TGFB1 (14/15 contrasts), TNF (13/15 contrasts), CSF2, Vegf (12/15 contrasts), TCF3, IL4, PTEN (11/15
455 contrasts). The contrast ZFU.20-0 presented 115 significant upstream regulators, while only eight and 13
456 were significantly enriched in BAO.20-0 and LAG.20-0 respectively; NDA.20-0 and BOR.20-0 displayed 86
457 and 87 significant upstream regulators respectively.

458 In order to visualize the main activated or inhibited regulators predicted by IPA according to the up- or
459 downregulation of the target DEGs, Fig 8 presents the estimated Z-scores of 61 upstream regulators with
460 significant p -values ($<10^{-6}$) and Z-scores ($|Z\text{-score}| \geq 2$) in at least one significant contrast. Among them, 29
461 upstream regulators, presenting positive Z-scores, were assessed as activated in some contrasts during
462 infection (top of Fig 8), 25 were roughly inhibited (middle of Fig 8), and 7 showed a dynamic pattern with
463 rather positive Z-scores at DIP.20 followed by negative Z-scores (bottom of Fig 8).

464
465

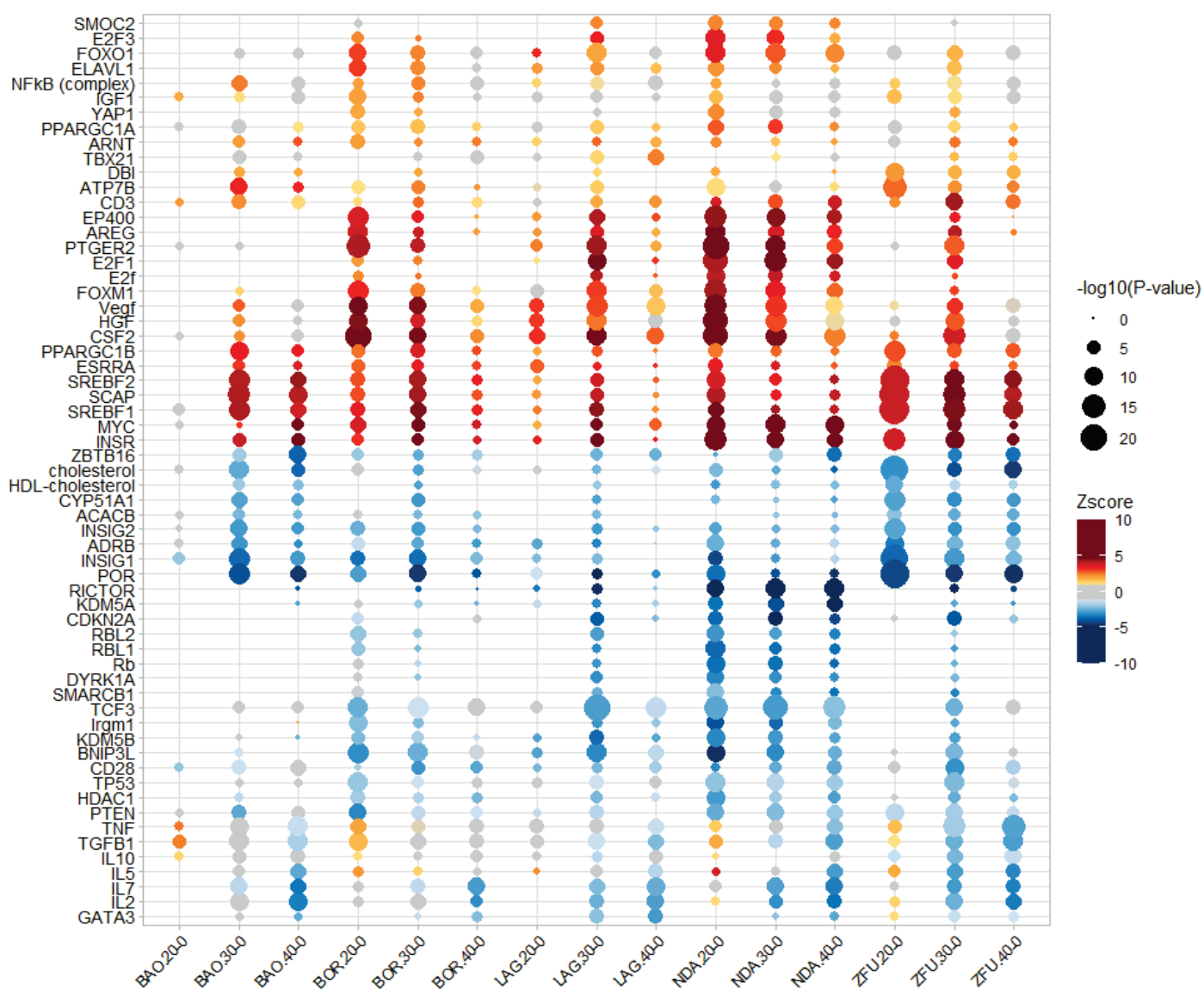


Figure 8. Plot of 61 significantly enriched upstream regulators inferred as activated or inhibited in function of the within-breed contrasts. The 15 within-breeds contrasts are shown on the abscissa and the significantly enriched diseases and functions on the ordinate. The size of the circles is inversely proportional to the P-value of the upstream regulator in the aforementioned contrast. The color gradient of the circle corresponds to the Z-score range, i.e. warm color gradient for positive Z-score > 1, cold color gradient for negative Z-score < -1, and gray color gradient for Z-scores ranging between -1 and 1.

466 ZFU was characterized by very high Z-scores and levels of significance during infection for SREBF2, SCAP,
467 and SREBF1. These upstream regulators were also significantly activated in the other breeds but not
468 constantly during infection. Interestingly, the SREBF2 gene itself was significantly and exclusively up-
469 regulated in ZFU contrasts. ATP7B was durably activated in ZFU, and temporarily in BAO and BOR. ZFU
470 displayed constantly inhibited upstream regulators: cholesterol, CYP51A1, ACACB, INSIG1, INSIG2, and
471 POR.

472 NDA was distinguished on Fig 8 by strong activation of CSF2, INSR, MYC, HGF, Vegf, and PTGER2. These
473 upstream regulators were also activated in the other breeds but with smaller intensities and durations. The
474 high inhibition of RICTOR was a unique feature of NDA, as well as that of KDM5A. The last three breeds,
475 BAO, BOR, and LAG, did not present striking features. The contrast BAO.30-0 shared similarities with

476 ZFU.20-0, naming high activation of SREBF1, SREBF2, and SCAP, and inhibition of INSIG1 and POR. BAO and
477 BOR presented an activation of NFkB (complex). BOR and LAG displayed similar features to NDA (e.g.,
478 strong activation of CSF2 or FOXO1). LAG only showed a significant activation of TBX21 and an inhibition of
479 GATA3 at DPI.40-0.

480 As upstream regulators, several cytokines (IL2, IL5, IL7, and TNF) and the growth factor TGFB1 showed
481 a dynamic pattern: they presented rather positive Z-scores at DPI.20 and were then assessed as
482 significantly inhibited at 30 or 40 DPI (bottom of Fig 8). TNF was significantly activated in BOR.20-0 and
483 significantly inhibited in NDA.40-0 and ZFU.40-0. Likewise, TGFB1 was activated in BAO.20-0 and inhibited
484 in NDA, ZFU and LAG at DPI.40. IL10 was significantly inhibited in ZFU.30-0.

485 **Some differentially expressed genes between NDA and ZFU before infection are differentially expressed
486 during infection**

487 Because NDA was the breed with the highest total number of DEGs during infection, and ZFU and NDA
488 presented some distinct enriched biological pathways, we decided to compare DEGs detected in the
489 contrast NDA.0-ZFU.0 to those identified during infection in the corresponding within-breed contrasts.
490 Among DEGs identified in the NDA.0-ZFU.0 contrast, 82 (53%) were also found DE during infection either
491 within NDA or within ZFU. A heatmap performed on the logFC of these 82 genes in the within-breed
492 contrasts shows that the first level of clustering was due to the separation between ZFU and the other
493 breeds, and the second level separated the early infection time point (DPI.20-0) from the others (S5 Fig).
494 The most upregulated genes during infection were MARCO (macrophage receptor with collagenous
495 structure, significantly upregulated in all breeds except ZFU during infection), and ENSBTAG00000022715
496 (unannotated gene in Ensembl). Conversely, IGF2 (Insulin-like Growth Factor 2) was downregulated in all
497 breeds, but especially in NDA, whereas ANKEF1 was significantly downregulated in NDA only.

498 Among these genes, 55 were involved in canonical pathways or biological functions that were enriched
499 during infection (S10 Table) and, among them, 25 were present in at least ten functions. Top represented
500 DEGs were IL2RA, which was involved in 276 functions, IGF2 in 142, GATA1 in 95, GPB2 in 52, and MARCO
501 in 58 functions. Thirty-three canonical pathways were concerned, among which oxidative phosphorylation,
502 mitochondrial dysfunction, sirtuin pathway, and Th1 and Th2 pathways. 351 diseases and functions
503 contained DEGs in NDA.0-ZFU.0, top functions in term of number of genes were in particular associated
504 with cancer, cell death and survival, cell movement, cell-to-cell signaling and interaction, hematological
505 disease and inflammatory response. At last, 105 upstream regulators could influence the expression of
506 genes among which some were DE between ZFU and NDA before infection. Top enriched upstream
507 regulators included cytokines (i.e., INF γ , IL2, TNF, CSF2, IL4), growth factors (TGFB1, HGF), TP53, Vegf and
508 MYC.

509 **Discussion**

510 Though bovine trypanotolerance has been described for more than a century (Pierre, 1906), the
511 biological bases of this phenotype remain poorly understood, due to the complexity of the trait that is
512 multigenic and multifactorial (dependent on environmental factors), and to the difficulty to perform
513 experimental infections on cattle, in comparison with model species (Morrison et al., 2016). In order to
514 increase knowledge on the physio-pathology of *T. congolense* infection in cattle, our study provides the
515 first whole blood transcriptome profiling using RNA-seq of five bovine breeds, including African taurine
516 shorthorn and longhorn, during an experimental trypanosome infection. The deep functional analysis of
517 the differentially expressed genes before and during infection identified new clues about trypanotolerance.
518 More precisely, our results confirmed and clarified some previous observations about the genes and the
519 main biological functions modulated during trypanosome infection in cattle (O'Gorman et al., 2006),
520 (O'Gorman et al., 2009). We observed a massive modification of the bovine transcriptome during *T.*
521 *congolense* infection in five West-African breeds, in accordance with the results of these previous
522 experiments that compared N'Dama and Boran breeds, notwithstanding that the experiments were done
523 on different cells (whole blood in the present study instead of Peripheral Blood Mononuclear Cells in
524 previous studies) using different techniques (RNA-seq in this study versus microarrays and/or qRT-PCR in

525 previous studies). In addition, the six genes (i.e., IL6, CCL2, IL10, IL1RN, IL8, NFKB1) DE in (O'Gorman et al.,
526 2006) and our study varied in the same direction, e.g., IL6 and NFKB1 were clearly upregulated, while IL1RN
527 was strongly downregulated in all breeds (except BOR). Among 23 DE genes representing various biological
528 processes and selected by (O'Gorman et al., 2009) for qRT-PCR validation, sixteen were also DE in the same
529 direction in our data set (eight upregulated and eight downregulated in both experiments, the remaining
530 seven being not significantly expressed in our data set or not annotated in Ensembl).

531 **A core transcriptomic response in blood cells of all five West-African breeds infected by *T. congolense***

532 Our global analysis of gene expression of blood cells and of their associated biological functions
533 completed previous works by showing that blood cell transcriptomes responded globally similarly to
534 trypanosome infection whatever the breed. Indeed, all breeds exhibited a parallel shift in their gene
535 expression profiling. A majority of DEGs (62.3%) were shared among at least two breeds, and fold-changes
536 of all DEGs common to two or more breeds varied in the same direction, except one gene (i.e., SPARC).
537 This core cattle transcriptomic response to trypanosome infection is a reminder that cattle, whatever the
538 breed, experience parasitemia waves and show symptoms (e.g., anemia), albeit at varying intensities and
539 durations depending on the breed, as observed in experiments (Berthier et al., 2015), (Authie et al., 1993),
540 (Naessens et al., 2003), (Van der Waaij et al., 2003), or in the field (Trail et al., 1994). The functional
541 annotation of the DEGs shared between breeds during infection also allowed us to provide a global picture
542 of the impact of infection on whole blood gene transcription, by identifying hematopoiesis and immune
543 response, and metabolism as the main gene functions targeted by *T. congolense* infection.

544 **Modulation of hematopoiesis and immune response during infection**

545 We detected in particular the modulation of gene transcription involved in hematopoiesis during
546 infection such as HBM, a highly upregulated DEG in all breeds. This increase of HBM expression suggests
547 that cattle responded quickly to cope with anemia induced by trypanosomes through an important supply
548 of reticulocytes from the bone marrow into the blood, while very low expression level of hemoglobin
549 subunits is normally found in the blood of healthy cattle (Correia et al., 2018). Expression of TFRC, an
550 important gene for erythropoiesis and also for T and B cell development and proliferation (Ned et al., 2003)
551 was also upregulated.

552 In addition, many top DEGs detected in all breeds are involved in immune response. Among them, five
553 (i.e., NR4A1, CCL22, IFI30, CTSZ and KYNU) out of the six genes significantly upregulated in all within-breeds
554 contrasts during infection are especially expressed in the monocyte lineage and/or dendritic cells (DC),
555 which initiate the immune response, presenting antigens to T lymphocytes (Wang et al., 2018), (Nowyhed
556 et al., 2015), (Vulcano et al., 2001), (Arunachalam et al., 2000), (Kos et al., 2005), (Harden et al., 2016),
557 (Obermajer et al., 2008). These cell types are known to be activated during trypanosomosis in cattle (Anosa
558 et al., 1999) and mice (Magez et al., 2007), and to play a decisive role in protection or pathology
559 (Bosschaerts et al., 2009). More specifically, NR4A1, a nuclear receptor with an inhibitory role in Th1 and
560 Th17 cell differentiation and in CD8 T cell expansion (Wang et al., 2018), (Nowyhed et al., 2015) could have
561 a protective role during trypanosomosis by modulating inflammation (Morias et al., 2015). As for IL17REL,
562 it was associated with inflammation and inflammatory diseases in human (Franke et al., 2010).

563 Additional common upregulated genes and enriched biological functions and upstream regulators
564 underlined the activation of innate immune response and macrophages, reported in cattle (Sileghem et al.,
565 1993), (Anosa et al., 1999), (Taiwo & Anosa, 2000), (Naessens, 2006) and mouse (Bosschaerts et al., 2009),
566 (Kuriakose et al., 2019). Indeed, important genes known to respond to pathogen stimuli and to trigger
567 immune response were found upregulated in all breeds during infection, such as MAPK11 and MAPK12
568 (Risco et al., 2012), NFKB1, up-regulated in bovine PBMC during trypanosomosis (O'Gorman et al., 2006),
569 and NFKB2. Activation of NF- κ B complex was shown in endothelial cells and macrophages during *in vitro*
570 interactions with trypanosomes where it promoted a pro-inflammatory response (Ammar et al., 2013),
571 (Leppert et al., 2007), but NF- κ Bp50 encoded by NFKB1 was also able to stimulate the production of the
572 anti-inflammatory cytokine IL-10 (Bosschaerts et al., 2011). Interestingly, a strongly up-regulated common
573 DEG was ARG1, which codes for arginase-1, a key enzyme of arginine metabolism mainly expressed in

574 macrophages and associated with ornithine production and inhibition of NO production (Mills et al., 2000).
575 ARG1 activity is induced in macrophages of mice infected by *T. brucei* (Gobert et al., 2000) or *T. congolense*
576 (Noel et al., 2002) and its expression level depends on the genetic background of trypanotolerant and
577 susceptible mice (Duleu et al., 2004), (Kierstein et al., 2006). In mice infected by *T. congolense*, ARG1 is
578 involved in immune suppression induced by myeloid-derived suppressor cells that impair proliferation and
579 INF-g production of CD4 T cells (Onyilagha et al., 2018). Moreover, arginase activity has a direct positive
580 impact on trypanosome growth through ornithine production (Fairlamb & Cerami, 1992), (De Muylder et
581 al., 2013). In our data set, ARG1 was found to be highly expressed during infection, similarly to what is
582 found in mice, but with no straightforward differences between breeds. Activation of DC and macrophages
583 may also be highlighted by down-regulated genes, like DAB2 (a Clathrin Adaptor Protein) that acts as an
584 intrinsic negative regulator of immune function and inflammation in those cells (Ahmed et al., 2015), (Hung
585 et al., 2016).

586 Macrophage activation was also highlighted by the enrichment of upstream regulators like CSF1 (highly
587 enriched and activated in the common DEGs) and CSF2 (highly enriched and activated in within-breed
588 contrasts), which are essential cytokines enhancing macrophage and DC survival and activation (Becher et
589 al., 2016), IFNG, shown to be essential in the early-stage control of trypanosomosis in the mouse (Magez
590 et al., 2020), and TNF, which changed from a rather activated state at DPI.20-0 to an inhibition state at
591 DPI.40-0 recalling the switch from pro-inflammatory macrophages to anti-inflammatory macrophages
592 highlighted in tolerant mouse models (De Baetselier et al., 2001). Looking globally at the results, common
593 DEGs were rather associated with an anti-inflammatory balance (e.g., ARG1), as exemplified by the function
594 inflammation of central nervous system which was inferred as inhibited. Nevertheless, it is speculative to
595 infer pro-inflammatory or anti-inflammatory macrophages from our data set, as macrophage populations
596 are particularly plastic in space and time, and genes associated with both types were regulated (e.g., CCL22,
597 ARG1, IL1R1, PDC1LG2 regulation fitted with anti-inflammatory macrophages, while IL16, NR1D2, DAB2,
598 IRF5, NFKB fitted with pro-inflammatory macrophages according to (Arango Duque & Descoteaux, 2014),
599 (Jablonski et al., 2015), (Murray, 2017)).

600 The functional annotation of DEGs common to the breeds also highlighted the enrichment of the
601 activation of B cells (with several upregulated common DEGs highly expressed in B cells, like CD19, CD22,
602 CD40, CD72, CD79B, and CD180), which was previously reported in cattle infected by *T. congolense* (Pinder
603 et al., 1988), (Naessens & Williams, 1992), (Taylor et al., 1996), (O'Gorman et al., 2009), in human (Boda et
604 al., 2009), (Lejon et al., 2014) and mouse (Onyilagha et al., 2015). In addition, we noticed an activation of
605 B Cell Receptor Signaling, PI3K Signaling in B Lymphocytes and Quantity of B-2 cells in which common DEGs
606 were involved, and an enrichment of Quantity of B Lymphocytes in all breeds from DPI.30.

607 Common DEGs and their functions were also related to T-cell-mediated immunity. We noticed a
608 downregulation of genes mainly expressed in T cells, or NK cells, like CD2, CD3D, CD3E, CD3G, CD7, CD27,
609 CD40L, CD225, CD247, and ZAP70, of IL16, a chemoattractant for CD4 T cells (Wilson et al., 2004), and of
610 LIF (Leukemia Inhibitory Factor), a pleiotropic cytokine expressed by T cells, especially CD4 T cells in human
611 and regulatory T cells in mouse (Metcalfe, 2011). T cell functions were inferred as strongly inhibited (e.g.,
612 T cell development, activation of T lymphocytes, T cell migration), especially from DPI.30. Moreover, IL2,
613 an upstream regulator of the common DEGs, was significantly inhibited from DPI.30 in NDA, ZFU and LAG,
614 and from DPI.40 in BAO and BOR, as previously observed in PBMC from infected NDA and Boran Zebu
615 (O'Gorman et al., 2006). This global result is in line with an impairment of T cell functions as previously
616 observed in infected cattle ((Flynn & Sileghem, 1991), (Sileghem & Flynn, 1992b)), suggested in HAT (Boda
617 et al., 2009), and reported in mouse (Uzonna et al., 1998).

618 If we underlined an inhibition of T cell functions during the chronic phase of the disease, our results
619 also suggest an activation in the earlier phase, as illustrated by the detection of an early activation of the T
620 cell co-receptor CD3 as an upstream regulator. Interestingly, CD3 gene expression may be negatively
621 regulated during T cell activation (Paillard et al., 1990), (Badran et al., 2005), (Krishnan et al., 2001) likely
622 by a negative feed-back system necessary to control this process. In addition, another surprising result was
623 the inferred inhibited state of IL7 as an upstream regulator of the common DEGs during infection, though,
624 at the mRNA level, IL7 expression was significantly and sustainably upregulated and IL7RA was significantly
625 downregulated, which is expected under T cell activation (Alves et al., 2008). Two hypotheses may be
626 proposed. First, since trypanosomes are capable of long-term survival in the vertebrate host thanks to

627 antigenic variation (Jackson et al., 2012), (Matthews et al., 2015), a reduced expression of IL7RA and a
628 resulting hyporesponsiveness to IL7 could constitute a protective way to avoid T cell over-activation.
629 Second, IL7 upregulation could be a consequence of T cell lymphopenia (Fry et al., 2001) due to
630 trypanosome factors (Cnops et al., 2015). Whether this dynamic is due to an immunosuppression induced
631 by trypanosomes, or a component of the host-parasite equilibrium (Taylor, 1998) to avoid a deleterious
632 sustained inflammatory response cannot be answered.

633 **Modulation of gene expression involved in metabolism during infection**

634 Among the main functions and biological processes identified as significantly enriched in DEGs detected
635 in all breeds during infection, functions related to metabolism are clearly highlighted. First, regulation of
636 lipid metabolism was highly impacted during infection, and could suggest a direct effect of trypanosomes
637 or a modulation of the host immune response (Kay et al., 2006), (Fessler, 2015). Indeed, several up-
638 regulated genes in all breeds were involved in cholesterol synthesis (e.g., MVD, ID1, FDFT1, SQLE, LSS,
639 CYP51A1), and accordingly, lipid metabolism functions (e.g., synthesis of cholesterol and sterol),
640 cholesterol biosynthesis and mevalonate pathways, and key upstream regulators of cholesterol synthesis
641 (SREBF1 and SREBF2, INSR) were strongly enriched and activated in the common DEGs data set, while
642 cholesterol, as an upstream regulator, was considered inhibited, thus promoting its own synthesis. If
643 previous studies suggested the involvement of lipid metabolism regulation in the physiopathology of AAT
644 in mice (Kierstein et al., 2006), in cattle and goat infected by *T. congolense* (Traore-Leroux et al., 1987),
645 (Meade et al., 2009), (Rajavel et al., 2020), (Ndoutamia et al., 2002), this is the first time that this
646 involvement has been detected to such an extent. Modification in lipid metabolism could be due to a direct
647 effect of trypanosomes that are able to internalize lipoproteins (Green et al., 2003), but it could also likely
648 reflect an activation of the inflammatory response as suggested by (Bouvier-Muller et al., 2017).

649 Second, the change observed in our study in the energy production of the cells probably reflects the
650 modification of immune cell energetic metabolism required to support cell growth, proliferation and
651 effector functions (Donnelly & Finlay, 2015) during infection by *T. congolense*. The tricarboxylic acid (TCA)
652 cycle, which is a hub for generating energy and building blocks for macromolecule synthesis as well as
653 releasing intra-cellular signaling molecules (Martinez-Reyes & Chandel, 2020), was indeed highly enriched
654 and activated in the common DEGs that we detected in our study and in some within-breeds contrasts.
655 Besides, gluconeogenesis and glycolysis were also assessed as activated during infection. These two
656 opposite pathways shared many genes whose corresponding proteins may catalyze reactions in two
657 directions. Nevertheless, since PKLR, involved in a key step for glycolysis, was upregulated in all the breeds
658 during infection, and that FBP1, responsible for final steps for gluconeogenesis (Lebigot et al., 2015), was
659 downregulated, we can suppose that glycolysis was actually the activated pathway during infection. These
660 results are concordant with the absence of gluconeogenesis in blood cells and with the interdependency
661 of glycolysis and TCA cycle, glycolysis supplying TCA cycle with pyruvate and providing molecules for
662 synthetizing nucleotides, glycerol and amino acids (Donnelly & Finlay, 2015).

663 **Breed-specific whole blood transcriptomic responses**

664 A focus on how each breed reacted to infection allowed observing some variations in their
665 transcriptome, in regard to the enrichment and intensity of activation or inhibition of some biological
666 functions. As previously reported by (O'Gorman et al., 2009), the blood transcriptome of NDA cattle, the
667 trypanotolerant breed of reference (Murray et al., 1984), (Hanotte et al., 2003), seemed to respond earlier
668 and more intensely to infection, with a higher number of detected DEGs in this breed during our
669 experiment in comparison with the other breeds, except at DPI.30-0 when LAG had a little more DEGs. In
670 addition, NDA harbored a more intense and earlier activation of several upstream regulators, notably
671 involved in immune response, in comparison with the other breeds, as exemplified by CSF2, the top
672 activated upstream regulator in NDA at DPI.20-0, that is a key cytokine produced by various cells during an
673 infection or an inflammation and involved in monocyte, macrophage, granulocyte and DC functions (Van
674 de Laar et al., 2012), (Hamilton & Achuthan, 2013). The highly estimated activation state of CSF2 in NDA in
675 our study could reflect an earlier and greater activation of macrophages in this breed, consistent with the

earlier release of co-stimulatory cytokines by NDA monocytes in comparison with Boran Zebu monocytes (Sileghem et al., 1993) and the hypothesis of an earlier pro-inflammatory response in PBMC from NDA (O'Gorman et al., 2006). PTGER2, the receptor of prostaglandin E2, an inflammation mediator (Kawahara et al., 2015) associated with a pro-inflammation profile in a mouse model of Chagas disease caused by *T. cruzi* (Guerrero et al., 2015), was also considered as highly and precociously activated. In NDA.30-0 and NDA.40-0 contrasts, MYC, activated in M2 macrophages (Pello et al., 2012), (Jablonski et al., 2015), and critical in T cell proliferation and growth following activation (Wang et al., 2011), was the most activated upstream regulator. We could thus hypothesize that trypanotolerance in NDA could be linked to the precocity and the chronology of activation state of cells, which would allow an efficient immune response while avoiding immune disorders (Vincendeau & Bouteille, 2006).

In addition, biological processes related to cell cycle and DNA metabolism (e.g., diseases and functions like segregation of chromosomes, metabolism of DNA; canonical pathways like cyclins and cell cycle regulation; upstream regulators like E2F1, FOXM1), were strongly enriched and activated in blood cells of NDA breed at DPI.20-0 and DPI.30-0, and explained the enrichment of functions linked to cancer. These results suggest an early activation of division and proliferation of some blood cell types in NDA (e.g., lymphocytes, (Naessens & Williams, 1992), (Naessens et al., 2003)). Curiously, like in all breeds, the lymphopoiesis function was assessed as strongly inhibited from DPI.30-0. These results could seem paradoxical but the sets of genes associated with lymphopoiesis on the one hand, and with cell cycle on the other hand, are different, the former function comprising DEGs encoding T cells surface antigens, cytokines receptors and signal transducers, and the latter comprising DEGs involved in mitosis and centromere formation.

Lastly, NDA displayed a particularly important shift in energetic metabolism of blood cells, whose fine tuning is associated with cell type and fate (O'Neill et al., 2016). Indeed, a key feature of NDA canonical pathways was the strong enrichment of oxidative phosphorylation and mitochondrial dysfunction, the former being highly activated such as TCA cycle and glycolysis. The fact that these three pathways were inferred as activated corroborates the presence of diverse immune cell populations and/or B cell activation. Indeed, glycolysis is rather associated with pro-inflammatory macrophages (Mills et al., 2016), activated DCs or effector T cells (McGettrick & O'Neill, 2013), while oxidative phosphorylation is rather associated with anti-inflammatory macrophages, Tregs or memory T cells (McGettrick & O'Neill, 2013), (Mills et al., 2016), and both seem increased in activated B cells (Caro-Maldonado et al., 2014). However, the strongest activation of oxidative phosphorylation observed in NDA could also be associated with a predominance of an anti-inflammatory component (Pearce & Pearce, 2013) during the chronic phase of infection at 30 and 40 DPI. Regulation of metabolic processes was also highlighted by the enrichment of the sirtuin signaling pathway, which was particularly significantly inhibited in NDA. This pathway comprises several proteins involved in ubiquitous processes and especially in a coupling between metabolic and stress factors and inflammatory response (Loftus & Finlay, 2016). In the same way, the most inhibited upstream regulator in NDA was the RICTOR protein that belongs to mTORC2 complex. The latter regulates cell metabolism and is involved in numerous functions, including development (Guertin et al., 2006), insulin signaling by promoting lipogenesis and glycogen synthesis (Yoon, 2017), and immune cell functions.

ZFU, which had the most pronounced anemia, the most durable parasitemia, and the lowest leukocytosis among the five breeds studied (Berthier et al., 2015), was characterized by a high enrichment and a strong activation/inhibition of biological functions, pathways and upstream regulators linked to lipid metabolism from the beginning of infection (i.e., synthesis of cholesterol, superpathway of cholesterol biosynthesis), which could interact with immune response. This was exemplified by SREBF2, a major transcription factor involved in cholesterol metabolism (Bommer & MacDougald, 2011), strongly activated as an upstream regulator, and also continuously upregulated in ZFU exclusively. In addition, the LXR/RXR activation pathway was found significantly enriched in ZFU but not in NDA nor LAG. Interestingly, (Morrison et al., 2010) identified this pathway as differentially enriched between mice infected by two *T. brucei* strains provoking distinct phenotypes. This pathway, notably expressed in hepatocytes and macrophages, is involved in lipid metabolism and innate immunity in macrophages (Joseph et al., 2004), (Ahsan et al., 2018), with rather an anti-inflammatory balance (Schulman, 2017). In the same direction, the significant inhibition of the inflammasome pathway at DPI.40 in ZFU only tended to show an inhibition of the inflammatory response at the chronic stage of infection in this breed (Zamboni & Lima-Junior, 2015).

729 LAG, whose trypanotolerance has been demonstrated (Berthier et al., 2015) (i.e., mild anemia and quick
730 recovery), showed a similar whole-blood transcriptome profile to NDA during the experiment (Fig 2). If LAG
731 had less DEGs than NDA, it responded relatively intensely to infection, especially at DPI.30-0, and most
732 information about functional analyses was found at this date. In LAG, like in NDA, top activated canonical
733 pathways were linked to cell energy production, i.e., oxidative phosphorylation and TCA Cycle,
734 mitochondrial dysfunction was enriched, and diseases and functions linked to cell cycle functions (G2/M
735 phase transition, Interphase, Segregation of chromosomes) were activated. Superpathway of cholesterol
736 biosynthesis was also activated, but, unlike the other breeds, not any disease and function linked to
737 cholesterol or lipid metabolism was significant. Top upstream regulators were also shared with NDA, as
738 CSF2, the most enriched and activated upstream regulator at DPI.20-0, and HGF, Vegf, MYC, INSR and TCF3.
739 More specific to LAG response, GATA3 and TBX21, reportedly expressed in an opposite way and
740 respectively associated with Th2 and Th1 cells (Chakir et al., 2003), were significantly detected as upstream
741 regulators in LAG.40-0. GATA3, down regulated in all breeds at the mRNA level, was assessed as inhibited
742 in LAG, and TBX21, upregulated in LAG only, as activated. TBX21 was also associated with NK cell
743 development and effector functions (Deng et al., 2015). In LAG, a pro-inflammatory activation of the Th1
744 cell subset or NK could be considered, but results from the diseases and functions analysis showed rather
745 an inhibition of T cells. Nevertheless, TBX21 being also expressed in B-cells precursors, contrary to GATA3
746 (Harashima et al., 2005) and being required in B cells for IFNG dependent switching in IgG2a production
747 (Mohr et al., 2010), other biological mechanisms could be involved.

748 The BAO breed had an unexpected global transcriptomic response in comparison with its
749 trypanotolerant status, given that this breed did not present a significantly different level of anemia from
750 those of NDA and LAG during infection (Berthier et al., 2015). Indeed, the differential expression between
751 the different times after infection and DPI.0 were smaller in BAO than in other breeds, as shown by the
752 PCA visualization (Fig 2) and the small numbers of DEGs detected in BAO during the infection process. This
753 discrepancy between its transcriptomic response and its trypanotolerant status was reflected at the
754 functional analysis. Indeed, the transcriptomic response in BAO showed similar features to that of ZFU
755 regarding DEGs involved in cholesterol and lipid metabolism, while it resembled NDA and LAG regarding
756 TCA cycle activation, control of Ig quantities and B Cell Receptor Signaling.

757 At last, BOR, an admixed breed between AFZ and AFT (Flori et al., 2014), displayed an expected global
758 transcriptomic response according to its intermediate phenotype between tolerant and susceptible breeds
759 concerning anemia, parasitemia and leucocyte counts (Berthier et al., 2015). The functional analyses of
760 DEGs did not reveal specific responses in BOR, except the activation in BOR.40-0 of RNA transcription.
761 Significant functions were indeed shared with other breeds, such as the M phase and the segregation of
762 chromosomes at 20 DPI, strongly enriched in NDA, or the canonical pathways linked to cholesterol
763 metabolism at DPI.30-0 more enriched in ZFU.

764 **765 Baseline transcriptomic differences between trypanotolerant and susceptible breeds point to genes that
could influence the outcome of infection**

766 The cross-referencing of the DEG between breeds before infection and within breeds during infection
767 could provide additional information on gene expression and functions associated with trypanotolerance.
768 Though the PCA supports the hypothesis that a majority of the differences in gene expression before
769 infection results from demographic history (see Fig 2), some differences could be adaptive (Whitehead &
770 Crawford, 2006). Indeed, eighty-two genes were DE between NDA and ZFU before infection and also
771 responded to infection in NDA and/or ZFU. Many of these genes are reported to be involved in functions
772 highlighted previously, e.g., immune response and metabolism. One hypothesis is that differences in basal
773 expression of these genes could underline different proportions of cell types or different states of cell
774 activation between breeds, which could play a role in subsequent pathogenic processes caused by
775 trypanosomes.

776 As illustration, several genes are known to be associated with macrophage functions. Among them,
777 MARCO, whose expression level was higher in ZFU than in NDA and LAG before infection, but was
778 subsequently significantly upregulated in all breeds except in ZFU, is a pattern recognition receptor on
779 macrophages surface involved in phagocytosis of various pathogens and the subsequent enhancement of

780 immune response and chemokines expression (Arredouani et al., 2004), (Bowdish et al., 2009), (Xu et al.,
781 2017). MMD (Monocyte to macrophage differentiation-associated) is a gene expressed during monocyte
782 differentiation and macrophage activation (Liu et al., 2012), and it was similarly upregulated in ZFU.0 in
783 comparison to NDA.0, and upregulated during the infection in NDA, LAG and BOR. SLC11A1 (syn. Nramp1)
784 is also a macrophage gene, and was upregulated in ZFU.0 versus NDA.0, but it was then downregulated in
785 ZFU during infection. The corresponding protein regulates iron homeostasis in macrophages and gene
786 variants are associated with disease susceptibility or resistance (Archer et al., 2015). In addition, IL2RA,
787 which is strongly expressed by Tregs, effector T cells (Banham et al., 2006), NK cells (Esin et al., 2013),
788 (Hamilton et al., 2017), and granulocytes in cattle (Zoldan et al., 2014) was more expressed in ZFU.0 in
789 comparison with the other breeds, and downregulated during infection and particularly in ZFU. IL2RA (syn.
790 CD25) has been the target of research in bovine trypanosomosis, where its impairment was noticed in
791 lymph nodes (Sileghem & Flynn, 1992a). In mice, injection of anti-CD25 antibodies before experimental
792 infections with *T. congolense* led to discordant results related to protection or pathogeny (Okwor et al.,
793 2012), (Guilliams et al., 2007). Other genes harboring basal differences in their expression level were
794 associated with metabolism regulation. For instance, IGF2, which was upregulated in NDA.0 versus ZFU.0
795 and was downregulated during the infection, codes for a peptide hormone that is involved in metabolism,
796 tissue development and maintenance and is downregulated during under-nutrition or hypoglycemia
797 (Livingstone & Borai, 2014).

798

799 In summary, our study provides the first transcriptome profiling of whole blood cells of five West-
800 African bovine breeds during a trypanosome infection using RNA-seq. In order to identify potential
801 similarities among African taurine cattle, overlooked trypanotolerant breeds (i.e., Lagune and Baoule) were
802 considered in addition to N'Dama, which accounts for the majority of the studies about cattle
803 trypanotolerance. We observed that trypanosome infection due to *T. congolense* has a major impact on
804 cattle blood transcriptome, whatever the breed and we provided a global transcriptomic picture of
805 infection. In accordance with previous results, a strong regulation of the immune system functions with an
806 early activation of innate immune response, followed by an activation of humoral response and an
807 inhibition of T cell functions at the chronic stage of infection were detected in all breeds.

808

809 Most importantly, we highlighted overlooked features, as a strong modification in lipid metabolism.
810 We mainly noticed an early regulation of the immune response in NDA, associated with a strong activation
811 of energy production by the cell, a strong enrichment and activation of oxidative phosphorylation in NDA
812 and LAG, and an activation of the TCA cycle in AFT breeds, which was not highlighted in ZFU. These
813 differences in cellular energy could be linked in AFT to better functions of some cell types, like M2
814 macrophages, memory T cells or activated B cells, and could represent a key to decipher trypanotolerance.
815 If some DEGs, functions and biological pathways were shared between AFT breeds during infection, our
816 results highlight also differences in gene expression dynamics in these three trypanotolerant breeds (as
817 exemplified by the singular transcriptomic profile of Baoule). This suggests that AFT breeds, although
818 subjected to the same selective pressure caused by trypanosomes, may have developed different
819 adaptation mechanisms. In addition, the trypanosusceptible breed ZFU presented several canonical
820 pathways linked to inflammation inhibited from DPI.30, which was not observed in the other breeds, and
821 the strongest modification in lipid metabolism regulation. It would be worth exploring other African zebu
822 breeds to confirm if this observation is a global feature of indicine breeds. Some genes, known to be
823 involved in immune response or metabolism, were differently expressed between breeds before infection
824 and within breeds during infection and raise the hypothesis that basal differences between breeds could
825 impact the outcome in infection.

826

827 Finally, our study provided new and valuable data to contribute to a better knowledge of African
828 livestock genomics (Kemp, 2019), (Kim et al., 2020), and to decipher the pathogenic process in bovine
829 trypanosomosis due to *T. congolense*. A comparable experiment using *T. vivax* or *T. brucei brucei* would be
830 worthwhile to verify whether host responses are similar regardless of the infecting species or not. Overall,
interactions between immune response and metabolism deserve to be deeply explored in cattle in order
to improve preventive and curative measures of AAT and also other infectious diseases.

831

Acknowledgements

832
833
834

This work was supported by the CIRAD - UMR AGAP HPC Data Center of the South Green Bioinformatics platform (<http://www.southgreen.fr/>). We thank Jean Nakhle for having corrected the English version of the manuscript.

835

Funding

836
837
838
839
840

This work was supported by the ANR grant n°2011 JSV6 001 01 (<http://www.agence-nationalerecherche.fr/>) and by the LabEx ParaFrap (ANR-11-LABX-0024). MGX acknowledges financial support from France Génomique National infrastructure, funded as part of “Investissement d’avenir” program managed by Agence Nationale pour la Recherche (contract ANR-10-INBS-09). The PhD grant of Moana Peylhard was supported by CIRAD PhD grant program and IRD.

841

Conflict of interest disclosure

842
843

The authors declare no conflicts of interest relating to the content of this article. Sophie Thévenon is a recommender for PCI Infections.

844

Data, script and code availability

845
846
847
848
849
850

Raw sequences data (fastq, count matrix, experimental design) will be publicly available at GEO (<https://www.ncbi.nlm.nih.gov/geo/>) under accession number GSE197108 upon publication.

Scripts and intermediate tables (DEG analysis, input tables for IPA® analyses, output tables from IPA® analyses) are publicly available in Cirad Dataverse under <https://doi.org/10.18167/DVN1/L9SHAX>. SNP genotypes of the experimental cattle are publicly available in Cirad Dataverse under <https://doi.org/10.18167/DVN1/APTZOC> and in WIDDE (<http://widde.toulouse.inra.fr/widde/>).

851

Supporting information availability

852
853

Tables and figures are in the supplementary tables and figures files. Legends are displayed at the bottom of each tables and figures.

854

S1 Table. Summary information on sequencing and mapping results.

855

S2 Table. LogFC and FDR of the 13,107 genes for the 15 within-breed contrasts during infection.

856

S3 Table. LogFC and FDR of the 13,107 genes for the 4 between-breed contrasts at DPI.0.

857

S4 Table. Upstream regulators significantly enriched in the between-breed contrasts at DPI.0

858

S5 Table. Diseases and functions enriched in the common DEGs in the within-breed contrasts.

859

S6 Table. Upstream regulators enriched in the common DEGs in the within-breed contrasts.

860

S7 Table. Cross table of the enriched diseases and functions in the 15 within-breed contrasts.

861

S8 Table. Cross table of the canonical pathways in the 15 within-breed contrasts.

862

S9 Table. Cross table of the upstream regulators in the 15 within-breed contrasts.

863

S10 Table. Cross table between the functional categories enriched during infection and the genes differentially expressed in the contrast NDA.0-ZFU.0.

865

S1 Figure. Proportion of uniquely mapped reads on the trypanosome genome depending on time points.

866

S2 Figure. Principal components analysis of 120 cattle RNA-seq libraries based on normalized genes counts.

867

S3 Figure. Venn diagram showing the intersection of genes identified as DE in the within-breed contrasts.

868

S4 Figure. Venn diagram showing the intersection of genes identified as DE in the between-breed contrasts.

869

S5 Figure. Heatmap on the logFC of a subset of 82 DE genes.

870

References

- 871 Ahmed MS, Byeon SE, Jeong Y, Miah MA, Salahuddin M, Lee Y, Park SS, Bae YS (2015) Dab2, a negative
872 regulator of DC immunogenicity, is an attractive molecular target for DC-based immunotherapy.
873 *Oncoimmunology*, **4**, e984550. <https://doi.org/10.4161/2162402X.2014.984550>
- 874 Ahsan F, Maertzdorf J, Guhlich-Bornhof U, Kaufmann SHE, Moura-Alves P (2018) IL-36/LXR axis modulates
875 cholesterol metabolism and immune defense to *Mycobacterium tuberculosis*. *Sci Rep*, **8**, 1520.
876 <https://doi.org/10.1038/s41598-018-19476-x>
- 877 Akol GW, Authie E, Pinder M, Moloo SK, Roelants GE, Murray M (1986) Susceptibility and immune
878 responses of zebu and taurine cattle of West Africa to infection with *Trypanosoma congolense*
879 transmitted by *Glossina morsitans centralis*. *Vet Immunol Immunopathol*, **11**, 361-373.
880 [https://doi.org/10.1016/0165-2427\(86\)90038-3](https://doi.org/10.1016/0165-2427(86)90038-3)
- 881 Alsan M (2015) The Effect of the TseTse Fly on African Development. *American Economic Review*, **105**, 382-
882 410. <https://doi.org/10.1257/aer.20130604>
- 883 Alvarez I, Perez-Pardal L, Traore A, Fernandez I, Goyache F (2015) Lack of haplotype structuring for two
884 candidate genes for trypanotolerance in cattle. *J Anim Breed Genet*.
885 <https://doi.org/10.1111/jbg.12181>
- 886 Alvarez I, Perez-Pardal L, Traore A, Fernandez I, Goyache F (2016) African Cattle do not Carry Unique
887 Mutations on the Exon 9 of the ARHGAP15 Gene. *Anim Biotechnol*, **27**, 9-12.
888 <https://doi.org/10.1080/10495398.2015.1053606>
- 889 Alves NL, van Leeuwen EM, Derkx IA, van Lier RA (2008) Differential regulation of human IL-7 receptor alpha
890 expression by IL-7 and TCR signaling. *J Immunol*, **180**, 5201-5210.
891 <https://doi.org/10.4049/jimmunol.180.8.5201>
- 892 Amene BM, Chime AB, Anika SM (1991) The production performance of imported friesian cattle under
893 heavy *Trypanosoma* challenge in a rain forest zone of Nigeria. *Br. vet. J.*, **147**, 274-282.
894 [https://doi.org/10.1016/0007-1935\(91\)90052-O](https://doi.org/10.1016/0007-1935(91)90052-O)
- 895 Ammar Z, Plazolles N, Baltz T, Coustou V (2013) Identification of trans-sialidases as a common mediator of
896 endothelial cell activation by African trypanosomes. *PLoS Pathog*, **9**, e1003710.
897 <https://doi.org/10.1371/journal.ppat.1003710>
- 898 Anosa VO, Logan-Henfrey LL, Wells CW (1999) The role of the bone marrow in bovine trypanotolerance II.
899 Macrophage function in *Trypanosoma congolense*-infected cattle. *Comparative Haematology
900 International*, **9**, 208-219. <https://doi.org/10.1007/BF02585507>
- 901 Arango Duque G, Descoteaux A (2014) Macrophage cytokines: involvement in immunity and infectious
902 diseases. *Front Immunol*, **5**, 491. <https://doi.org/10.3389/fimmu.2014.00491>
- 903 Archer NS, Nassif NT, O'Brien BA (2015) Genetic variants of SLC11A1 are associated with both autoimmune
904 and infectious diseases: systematic review and meta-analysis. *Genes Immun*, **16**, 275-283.
905 <https://doi.org/10.1038/gene.2015.8>
- 906 Arredouani M, Yang Z, Ning Y, Qin G, Soininen R, Tryggvason K, Kobzik L (2004) The scavenger receptor
907 MARCO is required for lung defense against pneumococcal pneumonia and inhaled particles. *J Exp
908 Med*, **200**, 267-272. <https://doi.org/10.1084/jem.20040731>
- 909 Arunachalam B, Phan UT, Geuze HJ, Cresswell P (2000) Enzymatic reduction of disulfide bonds in lysosomes:
910 characterization of a gamma-interferon-inducible lysosomal thiol reductase (GILT). *Proc Natl Acad
911 Sci U S A*, **97**, 745-750. <https://doi.org/10.1073/pnas.97.2.745>
- 912 Authie E, Muteti DK, Williams DJ (1993) Antibody responses to invariant antigens of *Trypanosoma
913 congolense* in cattle of differing susceptibility to trypanosomiasis. *Parasite Immunol*, **15**, 101-111.
914 <https://doi.org/10.1111/j.1365-3024.1993.tb00589.x>
- 915 Badran BM, Kunstman K, Stanton J, Moschitta M, Zerghe A, Akl H, Burny A, Wolinsky SM, Willard-Gallo KE
916 (2005) Transcriptional regulation of the human CD3 gamma gene: the TATA-less CD3 gamma
917 promoter functions via an initiator and contiguous Sp-binding elements. *J Immunol*, **174**, 6238-
918 6249. <https://doi.org/10.4049/jimmunol.174.10.6238>
- 919 Banham AH, Powrie FM, Suri-Payer E (2006) FOXP3+ regulatory T cells: Current controversies and future
920 perspectives. *Eur J Immunol*, **36**, 2832-2836. <https://doi.org/10.1002/eji.200636459>

- 921 Becher B, Tugues S, Greter M (2016) GM-CSF: From Growth Factor to Central Mediator of Tissue
922 Inflammation. *Immunity*, **45**, 963-973. <https://doi.org/10.1016/j.immuni.2016.10.026>
- 923 Benjamini Y, Hochberg Y (1995) Controlling the false discovery rate: a practical and powerful approach to
924 multiple testing. *J R Stat Soc Series B Stat Methodol*, **57**, 289-300. <https://doi.org/10.1111/j.2517-6161.1995.tb02031.x>
- 925 Berthier D, Peylhard M, Dayo GK, Flori L, Sylla S, Bolly S, Sakande H, Chantal I, Thevenon S (2015) A
926 comparison of phenotypic traits related to trypanotolerance in five west african cattle breeds. *PLoS One*, **10**, e0126498.
927 <https://doi.org/10.1371/journal.pone.0126498>
- 928 Boda C, Courtioux B, Roques P, Pervieux L, Vatunga G, Josenando T, Ayenengoye CR, Bouteille B, Jauberteau
929 MO, Bisser S (2009) Immunophenotypic lymphocyte profiles in human african trypanosomiasis.
930 *PLoS One*, **4**, e6184. <https://doi.org/10.1371/journal.pone.0006184>
- 931 Bommer GT, MacDougald OA (2011) Regulation of lipid homeostasis by the bifunctional SREBF2-miR33a
932 locus. *Cell Metab*, **13**, 241-247. <https://doi.org/10.1016/j.cmet.2011.02.004>
- 933 Bosschaerts T, Guilliams M, Stijlemans B, De Baetselier P, Beschin A (2009) Understanding the role of
934 monocytic cells in liver inflammation using parasite infection as a model. *Immunobiology*, **214**,
935 737-747. <https://doi.org/10.1016/j.imbio.2009.06.010>
- 936 Bosschaerts T, Morias Y, Stijlemans B, Herin M, Porta C, Sica A, Mantovani A, De Baetselier P, Beschin A
937 (2011) IL-10 limits production of pathogenic TNF by M1 myeloid cells through induction of nuclear
938 NF-kappaB p50 member in *Trypanosoma congolense* infection-resistant C57BL/6 mice. *Eur J
939 Immunol*, **41**, 3270-3280. <https://doi.org/10.1002/eji.201041307>
- 940 Bouvier-Muller J, Allain C, Tabouret G, Enjalbert F, Portes D, Noirot C, Rupp R, Foucras G (2017) Whole
941 blood transcriptome analysis reveals potential competition in metabolic pathways between
942 negative energy balance and response to inflammatory challenge. *Scientific reports*, **7**, 2379
- 943 Bouyer J, Bouyer F, Donadeu M, Rowan T, Napier G (2013) Community- and farmer-based management of
944 animal African trypanosomosis in cattle. *Trends Parasitol*, **29**, 519-522.
945 <https://doi.org/10.1016/j.pt.2013.08.003>
- 946 Bowdish DM, Sakamoto K, Kim MJ, Kroos M, Mukhopadhyay S, Leifer CA, Tryggvason K, Gordon S, Russell
947 DG (2009) MARCO, TLR2, and CD14 are required for macrophage cytokine responses to
948 mycobacterial trehalose dimycolate and *Mycobacterium tuberculosis*. *PLoS Pathog*, **5**, e1000474.
949 <https://doi.org/10.1371/journal.ppat.1000474>
- 950 Bradley DG, MacHugh DE, Cunningham P, Loftus RT (1996) Mitochondrial diversity and the origins of
951 African and European cattle. *Proc Natl Acad Sci U S A*, **93**, 5131-5135.
952 <https://doi.org/10.1073/pnas.93.10.5131>
- 953 Budd LT (1999) *DFID-funded tsetse and trypanosomiasis research and development since 1980*. Economic
954 Analysis (Vol. 2). Department of International Development, UK, London.
- 955 Caro-Maldonado A, Wang R, Nichols AG, Kuraoka M, Milasta S, Sun LD, Gavin AL, Abel ED, Kelsoe G, Green
956 DR, Rathmell JC (2014) Metabolic reprogramming is required for antibody production that is
957 suppressed in anergic but exaggerated in chronically BAFF-exposed B cells. *J Immunol*, **192**, 3626-
958 3636. <https://doi.org/10.4049/jimmunol.1302062>
- 959 Chakir H, Wang H, Lefebvre DE, Webb J, Scott FW (2003) T-bet/GATA-3 ratio as a measure of the Th1/Th2
960 cytokine profile in mixed cell populations: predominant role of GATA-3. *J Immunol Methods*, **278**,
961 157-169. [https://doi.org/10.1016/S0022-1759\(03\)00200-X](https://doi.org/10.1016/S0022-1759(03)00200-X)
- 962 Chen Y, Lun ATL, Smyth GK (2014) Differential expression analysis of complex RNA-seq experiments using
963 edgeR. In: *Statistical Analysis of Next Generation Sequence Data* (ed. Nettleton SDaDS), pp. 51-74.
964 Springer, New York.
- 965 CIPEA (1979) *Le bétail trypanotolérant d'Afrique occidentale et centrale* (Vol. 2), Addis Abeba, Ethiopie.
- 966 Cnops J, De Trez C, Stijlemans B, Keirsse J, Kauffmann F, Barkhuizen M, Keeton R, Boon L, Brombacher F,
967 Magez S (2015) NK-, NKT- and CD8-Derived IFNgamma drives myeloid cell activation and
968 erythrophagocytosis, resulting in trypanosomiasis-associated acute anemia. *PLoS Pathog*, **11**,
969 e1004964. <https://doi.org/10.1371/journal.ppat.1004964>
- 970 Correia CN, McLoughlin KE, Nalpas NC, Magee DA, Browne JA, Rue-Albrecht K, Gordon SV, MacHugh DE
971 (2018) RNA Sequencing (RNA-Seq) reveals extremely low levels of reticulocyte-derived globin gene

- 974 transcripts in peripheral blood from horses (*Equus caballus*) and cattle (*Bos taurus*). *Front Genet*,
975 9, 278. <https://doi.org/10.3389/fgene.2018.00278>
- 976 De Baetselier PD, Namangala B, Noel W, Brys L, Pays E, Beschin A (2001) Alternative versus classical
977 macrophage activation during experimental African trypanosomosis. *Int J Parasitol*, **31**, 575-587.
978 [https://doi.org/10.1016/S0020-7519\(01\)00170-9](https://doi.org/10.1016/S0020-7519(01)00170-9)
- 979 De Muylder G, Daulouede S, Lecordier L, Uzureau P, Morias Y, Van Den Abbeele J, Caljon G, Herin M,
980 Holzmuller P, Semballa S, Courtois P, Vanhamme L, Stijlemans B, De Baetselier P, Barrett MP,
981 Barlow JL, McKenzie AN, Barron L, Wynn TA, Beschin A, Vincendeau P, Pays E (2013) A
982 *Trypanosoma brucei* kinesin heavy chain promotes parasite growth by triggering host arginase
983 activity. *PLoS Pathog*, **9**, e1003731. <https://doi.org/10.1371/journal.ppat.1003731>
- 984 Deng Y, Kerdiles Y, Chu J, Yuan S, Wang Y, Chen X, Mao H, Zhang L, Zhang J, Hughes T, Deng Y, Zhang Q,
985 Wang F, Zou X, Liu CG, Freud AG, Li X, Caligiuri MA, Vivier E, Yu J (2015) Transcription factor Foxo1
986 is a negative regulator of natural killer cell maturation and function. *Immunity*, **42**, 457-470.
987 <https://doi.org/10.1016/j.jimmuni.2015.02.006>
- 988 Dobin A, Davis CA, Schlesinger F, Drenkow J, Zaleski C, Jha S, Batut P, Chaisson M, Gingeras TR (2013) STAR:
989 ultrafast universal RNA-seq aligner. *Bioinformatics*, **29**, 15-21.
990 <https://doi.org/10.1093/bioinformatics/bts635>
- 991 Doko A, Verhulst A, Pandey VS, Van der Stuyft P (1997) Trypanosomose expérimentale à *Trypanosoma*
992 *brucei brucei* chez les taurins Holsteins et les zébus Bororo blancs. *Revue Elev. Méd. vét. Pays trop.*,
993 **50**, 23-28. <https://doi.org/10.19182/remvt.9597>
- 994 Donnelly RP, Finlay DK (2015) Glucose, glycolysis and lymphocyte responses. *Mol Immunol*, **68**, 513-519.
995 <https://doi.org/10.1016/j.molimm.2015.07.034>
- 996 Duleu S, Vincendeau P, Courtois P, Semballa S, Lagroye I, Daulouede S, Boucher JL, Wilson KT, Veyret B,
997 Gobert AP (2004) Mouse strain susceptibility to trypanosome infection: an arginase-dependent
998 effect. *J Immunol*, **172**, 6298-6303. <https://doi.org/10.4049/jimmunol.172.10.6298>
- 999 Esin S, Counoupas C, Aulicino A, Brancatisano FL, Maisetta G, Bottai D, Di Luca M, Florio W, Campa M,
1000 Batoni G (2013) Interaction of *Mycobacterium tuberculosis* cell wall components with the human
1001 natural killer cell receptors NKp44 and Toll-like receptor 2. *Scand J Immunol*, **77**, 460-469.
1002 <https://doi.org/10.1111/sji.12052>
- 1003 Fairlamb AH, Cerami A (1992) Metabolism and functions of trypanothione in the Kinetoplastida. *Annu Rev
1004 Microbiol*, **46**, 695-729. <https://doi.org/10.1146/annurev.mi.46.100192.003403>
- 1005 Fessler MB (2015) Regulation of Adaptive Immunity in Health and Disease by Cholesterol Metabolism. *Curr
1006 Allergy Asthma Rep*, **15**, 48. <https://doi.org/10.1007/s11882-015-0548-7>
- 1007 Flori L, Thevenon S, Dayo GK, Senou M, Sylla S, Berthier D, Moazami-Goudarzi K, Gautier M (2014) Adaptive
1008 admixture in the West African bovine hybrid zone: insight from the Borgou population. *Mol Ecol*,
1009 **23**, 3241-3257. <https://doi.org/10.1111/mec.12816>
- 1010 Flynn JN, Sileghem M (1991) The role of the macrophage in induction of immunosuppression in
1011 *Trypanosoma congolense*-infected cattle. *Immunology*, **74**, 310-316
- 1012 Franke A, Balschun T, Sina C, Ellinghaus D, Hasler R, Mayr G, Albrecht M, Wittig M, Buchert E, Nikolaus S,
1013 Gieger C, Wichmann HE, Sventoraityte J, Kupcinskas L, Onnie CM, Gazouli M, Anagnou NP,
1014 Strachan D, McArdle WL, Mathew CG, Rutgeerts P, Vermeire S, Vatn MH, group Is, Krawczak M,
1015 Rosenstiel P, Karlsen TH, Schreiber S (2010) Genome-wide association study for ulcerative colitis
1016 identifies risk loci at 7q22 and 22q13 (IL17REL). *Nat Genet*, **42**, 292-294.
1017 <https://doi.org/10.1038/ng.553>
- 1018 Fry TJ, Christensen BL, Komschlies KL, Gress RE, Mackall CL (2001) Interleukin-7 restores immunity in
1019 athymic T-cell-depleted hosts. *Blood*, **97**, 1525-1533. <https://doi.org/10.1182/blood.v97.6.1525>
- 1020 Gobert AP, Daulouede S, Lepoivre M, Boucher JL, Bouteille B, Buguet A, Cespuglio R, Veyret B, Vincendeau
1021 P (2000) L-Arginine availability modulates local nitric oxide production and parasite killing in
1022 experimental trypanosomiasis. *Infect Immun*, **68**, 4653-4657.
1023 <https://doi.org/10.1128/IAI.68.8.4653-4657.2000>
- 1024 Green HP, Del Pilar Molina Portela M, St Jean EN, Lugli EB, Raper J (2003) Evidence for a *Trypanosoma*
1025 *brucei* lipoprotein scavenger receptor. *J Biol Chem*, **278**, 422-427.
1026 <https://doi.org/10.1074/jbc.M207215200>

- 1027 Guerrero NA, Camacho M, Vila L, Iniguez MA, Chillon-Marinas C, Cuervo H, Poveda C, Fresno M, Girones N
1028 (2015) Cyclooxygenase-2 and Prostaglandin E2 Signaling through Prostaglandin Receptor EP-2
1029 Favor the Development of Myocarditis during Acute *Trypanosoma cruzi* Infection. *PLoS Negl Trop*
1030 *Dis*, **9**, e0004025. <https://doi.org/10.1371/journal.pntd.0004025>
- 1031 Guertin DA, Stevens DM, Thoreen CC, Burds AA, Kalaany NY, Moffat J, Brown M, Fitzgerald KJ, Sabatini DM
1032 (2006) Ablation in mice of the mTORC components raptor, rictor, or mLST8 reveals that mTORC2
1033 is required for signaling to Akt-FOXO and PKC α , but not S6K1. *Dev Cell*, **11**, 859-871.
1034 <https://doi.org/10.1016/j.devcel.2006.10.007>
- 1035 Guilliams M, Oldenhove G, Noel W, Herin M, Brys L, Loi P, Flamand V, Moser M, De Baetselier P, Beschin A
1036 (2007) African trypanosomiasis: naturally occurring regulatory T cells favor trypanotolerance by
1037 limiting pathology associated with sustained type 1 inflammation. *J Immunol*, **179**, 2748-2757.
1038 <https://doi.org/10.4049/jimmunol.179.5.2748>
- 1039 Hamilton CA, Mahan S, Bell CR, Villarreal-Ramos B, Charleston B, Entrican G, Hope JC (2017) Frequency and
1040 phenotype of natural killer cells and natural killer cell subsets in bovine lymphoid compartments
1041 and blood. *Immunology*, **151**, 89-97. <https://doi.org/10.1111/imm.12708>
- 1042 Hamilton JA, Achuthan A (2013) Colony stimulating factors and myeloid cell biology in health and disease.
1043 *Trends Immunol*, **34**, 81-89. <https://doi.org/10.1016/j.it.2012.08.006>
- 1044 Hanotte O, Bradley DG, Ochieng JW, Verjee Y, Hill EW, Rege JE (2002) African pastoralism: genetic imprints
1045 of origins and migrations. *Science*, **296**, 336-339. <https://doi.org/10.1126/science.1069878>
- 1046 Hanotte O, Ronin Y, Agaba M, Nilsson P, Gelhaus A, Horstmann R, Sugimoto Y, Kemp S, Gibson J, Korol A,
1047 Soller M, Teale A (2003) Mapping of quantitative trait loci controlling trypanotolerance in a cross
1048 of tolerant West African N'Dama and susceptible East African Boran cattle. *Proc Natl Acad Sci U S*
1049 **A**, **100**, 7443-7448. <https://doi.org/10.1073/pnas.1232392100>
- 1050 Harashima A, Matsuo Y, Drexler HG, Okochi A, Motoda R, Tanimoto M, Orita K (2005) Transcription factor
1051 expression in B-cell precursor-leukemia cell lines: preferential expression of T-bet. *Leuk Res*, **29**,
1052 841-848. <https://doi.org/10.1016/j.leukres.2004.12.010>
- 1053 Harden JL, Lewis SM, Lish SR, Suarez-Farinias M, Gareau D, Lentini T, Johnson-Huang LM, Krueger JG, Lowes
1054 MA (2016) The tryptophan metabolism enzyme L-kynureninase is a novel inflammatory factor in
1055 psoriasis and other inflammatory diseases. *J Allergy Clin Immunol*, **137**, 1830-1840.
1056 <https://doi.org/10.1016/j.jaci.2015.09.055>
- 1057 Hung WS, Ling P, Cheng JC, Chang SS, Tseng CP (2016) Disabled-2 is a negative immune regulator of
1058 lipopolysaccharide-stimulated Toll-like receptor 4 internalization and signaling. *Sci Rep*, **6**, 35343.
1059 <https://doi.org/10.1038/srep35343>
- 1060 Jablonski KA, Amici SA, Webb LM, Ruiz-Rosado Jde D, Popovich PG, Partida-Sanchez S, Guerau-de-Arellano
1061 M (2015) Novel Markers to Delineate Murine M1 and M2 Macrophages. *PLoS One*, **10**, e0145342.
1062 <https://doi.org/10.1371/journal.pone.0145342>
- 1063 Jackson AP, Berry A, Aslett M, Allison HC, Burton P, Vavrova-Anderson J, Brown R, Browne H, Corton N,
1064 Hauser H, Gamble J, Gilderthorp R, Marcello L, McQuillan J, Otto TD, Quail MA, Sanders MJ, van
1065 Tonder A, Ginger ML, Field MC, Barry JD, Hertz-Fowler C, Berriman M (2012) Antigenic diversity is
1066 generated by distinct evolutionary mechanisms in African trypanosome species. *Proc Natl Acad Sci*
1067 **USA**, **109**, 3416-3421. <https://doi.org/10.1073/pnas.1117313109>
- 1068 Joseph SB, Bradley MN, Castrillo A, Bruhn KW, Mak PA, Pei L, Hogenesch J, O'Connell R M, Cheng G, Saez
1069 E, Miller JF, Tontonoz P (2004) LXR-dependent gene expression is important for macrophage
1070 survival and the innate immune response. *Cell*, **119**, 299-309.
1071 <https://doi.org/10.1016/j.cell.2004.09.032>
- 1072 Kawahara K, Hohjoh H, Inazumi T, Tsuchiya S, Sugimoto Y (2015) Prostaglandin E2-induced inflammation:
1073 Relevance of prostaglandin E receptors. *Biochim Biophys Acta*, **1851**, 414-421.
1074 <https://doi.org/10.1016/j.bbapap.2014.07.008>
- 1075 Kay JG, Murray RZ, Pagan JK, Stow JL (2006) Cytokine secretion via cholesterol-rich lipid raft-associated
1076 SNAREs at the phagocytic cup. *J Biol Chem*, **281**, 11949-11954.
1077 <https://doi.org/10.1074/jbc.M600857200>
- 1078 Kemp S (2019) Why science matters. African cattle in the genomic century. In: *The story of cattle in Africa: Why diversity matters* eds Dessie T & Mwai O), pp. 268. International Livestock Research Institute,
1079

- 1080 Rural Development Administration of the Republic of Korea and the African Union-InterAfrican,
1081 Bureau for Animal Resources, Nairobi, Kenya.

1082 Kierstein S, Noyes H, Naessens J, Nakamura Y, Pritchard C, Gibson J, Kemp S, Brass A (2006) Gene expression
1083 profiling in a mouse model for African trypanosomiasis. *Genes Immun*, **7**, 667-679.
1084 <https://doi.org/10.1038/sj.gene.6364345>

1085 Kim K, Kwon T, Dessie T, Yoo D, Mwai OA, Jang J, Sung S, Lee S, Salim B, Jung J, Jeong H, Tarekegn GM,
1086 Tijjani A, Lim D, Cho S, Oh SJ, Lee HK, Kim J, Jeong C, Kemp S, Hanotte O, Kim H (2020) The mosaic
1087 genome of indigenous African cattle as a unique genetic resource for African pastoralism. *Nat Genet*, **52**, 1099-1110. <https://doi.org/10.1038/s41588-020-0694-2>

1088 Kos J, Sekirnik A, Premzl A, Zavasnik Bergant V, Langerholc T, Turk B, Werle B, Golouh R, Repnik U, Jeras M,
1089 Turk V (2005) Carboxypeptidases cathepsins X and B display distinct protein profile in human cells
1090 and tissues. *Exp Cell Res*, **306**, 103-113. <https://doi.org/10.1016/j.yexcr.2004.12.006>

1091 Kramer A, Green J, Pollard J, Jr., Tugendreich S (2014) Causal analysis approaches in Ingenuity Pathway
1092 Analysis. *Bioinformatics*, **30**, 523-530. <https://doi.org/10.1093/bioinformatics/btt703>

1093 Krishnan S, Warke VG, Nambiar MP, Wong HK, Tsokos GC, Farber DL (2001) Generation and biochemical
1094 analysis of human effector CD4 T cells: alterations in tyrosine phosphorylation and loss of CD3zeta
1095 expression. *Blood*, **97**, 3851-3859. <https://doi.org/10.1182/blood.V97.12.3851>

1096 Kuriakose S, Onyilagha C, Singh R, Olayinka-Adefemi F, Jia P, Uzonna JE (2019) TLR-2 and MyD88-Dependent
1097 Activation of MAPK and STAT Proteins Regulates Proinflammatory Cytokine Response and
1098 Immunity to Experimental *Trypanosoma congolense* Infection. *Frontiers in immunology*, **10**, 2673.
1099 <https://doi.org/10.3389/fimmu.2019.02673>

1100 Le Cao K-A, Rohart F, Gonzales I, Dejean S, Gautier B, Bartolo F, Monget P, Coquery J, Yao F, Liquet B. (2016).
1101 mixOmics: Omics Data Integration Project. Retrieved from R package version 6.1.1.
1102 <https://CRAN.R-project.org/package=mixOmics>

1103 Lebigot E, Brassier A, Zater M, Imanci D, Feillet F, Therond P, de Lonlay P, Boutron A (2015) Fructose 1,6-
1104 bisphosphatase deficiency: clinical, biochemical and genetic features in French patients. *J Inherit
1105 Metab Dis*, **38**, 881-887. <https://doi.org/10.1007/s10545-014-9804-6>

1106 Lejon V, Mumba Ngoyi D, Kestens L, Boel L, Barbe B, Kande Betu V, van Griensven J, Bottieau E, Muyembe
1107 Tamfum JJ, Jacobs J, Buscher P (2014) Gambiense human african trypanosomiasis and
1108 immunological memory: effect on phenotypic lymphocyte profiles and humoral immunity. *PLoS
1109 Pathog*, **10**, e1003947. <https://doi.org/10.1371/journal.ppat.1003947>

1110 Leppert BJ, Mansfield JM, Paulnock DM (2007) The soluble variant surface glycoprotein of African
1111 trypanosomes is recognized by a macrophage scavenger receptor and induces I kappa B alpha
1112 degradation independently of TRAF6-mediated TLR signaling. *J Immunol*, **179**, 548-556.
1113 <https://doi.org/10.4049/jimmunol.179.1.548>

1114 Li H, Handsaker B, Wysoker A, Fennell T, Ruan J, Homer N, Marth G, Abecasis G, Durbin R, Genome Project
1115 Data Processing S (2009) The Sequence Alignment/Map format and SAMtools. *Bioinformatics*, **25**,
1116 2078-2079. <https://doi.org/10.1093/bioinformatics/btp352>

1117 Liao Y, Smyth GK, Shi W (2014) featureCounts: an efficient general purpose program for assigning sequence
1118 reads to genomic features. *Bioinformatics*, **30**, 923-930.
1119 <https://doi.org/10.1093/bioinformatics/btt656>

1120 Liu Q, Zheng J, Yin DD, Xiang J, He F, Wang YC, Liang L, Qin HY, Liu L, Liang YM, Han H (2012) Monocyte to
1121 macrophage differentiation-associated (MMD) positively regulates ERK and Akt activation and
1122 TNF-alpha and NO production in macrophages. *Mol Biol Rep*, **39**, 5643-5650.
1123 <https://doi.org/10.1007/s11033-011-1370-5>

1124 Livingstone C, Borai A (2014) Insulin-like growth factor-II: its role in metabolic and endocrine disease. *Clin
1125 Endocrinol (Oxf)*, **80**, 773-781. <https://doi.org/10.1111/cen.12446>

1126 Loftus RM, Finlay DK (2016) Immunometabolism: Cellular Metabolism Turns Immune Regulator. *J Biol
1127 Chem*, **291**, 1-10. <https://doi.org/10.1074/jbc.R115.693903>

1128 Loftus RT, MacHugh DE, Ngere LO, Balain DS, Badi AM, Bradley DG, Cunningham EP (1994) Mitochondrial
1129 genetic variation in European, African and Indian cattle populations. *Anim Genet*, **25**, 265-271.
1130 <https://doi.org/10.1111/j.1365-2052.1994.tb00203.x>

1131

- 1132 Magez S, Pinto Torres JE, Obishakin E, Radwanska M (2020) Infections With Extracellular Trypanosomes
1133 Require Control by Efficient Innate Immune Mechanisms and Can Result in the Destruction of the
1134 Mammalian Humoral Immune System. *Front Immunol*, **11**, 382.
1135 <https://doi.org/10.3389/fimmu.2020.00382>
- 1136 Magez S, Radwanska M, Drennan M, Fick L, Baral TN, Allie N, Jacobs M, Nedospasov S, Brombacher F, Ryffel
1137 B, De Baetselier P (2007) Tumor necrosis factor (TNF) receptor-1 (TNFp55) signal transduction and
1138 macrophage-derived soluble TNF are crucial for nitric oxide-mediated *Trypanosoma congolense*
1139 parasite killing. *J Infect Dis*, **196**, 954-962. <https://doi.org/10.1086/520815>
- 1140 Magez S, Radwanska M, Drennan M, Fick L, Baral TN, Brombacher F, De Baetselier P (2006) Interferon-
1141 gamma and nitric oxide in combination with antibodies are key protective host immune factors
1142 during *Trypanosoma congolense* Tc13 Infections. *J Infect Dis*, **193**, 1575-1583.
1143 <https://doi.org/10.1086/503808>
- 1144 Martinez-Reyes I, Chandel NS (2020) Mitochondrial TCA cycle metabolites control physiology and disease.
1145 *Nat Commun*, **11**, 102. <https://doi.org/10.1038/s41467-019-13668-3>
- 1146 Matthews KR, McCulloch R, Morrison LJ (2015) The within-host dynamics of African trypanosome
1147 infections. *Philos Trans R Soc Lond B Biol Sci*, **370**. <https://doi.org/10.1098/rstb.2014.0288>
- 1148 Mattioli RC, Feldmann U, Hendrickx G, Wint W, Jannin J, Slingenbergh J (2004) Tsetse and trypanosomiasis
1149 intervention policies supporting sustainable animal-agricultural development. *Journal of Food
1150 Agriculture & Environment*, **2**, 310-314
- 1151 McCarthy DJ, Chen Y, Smyth GK (2012) Differential expression analysis of multifactor RNA-Seq experiments
1152 with respect to biological variation. *Nucleic Acids Res*, **40**, 4288-4297.
1153 <https://doi.org/10.1093/nar/gks042>
- 1154 McGettrick AF, O'Neill LA (2013) How metabolism generates signals during innate immunity and
1155 inflammation. *J Biol Chem*, **288**, 22893-22898. <https://doi.org/10.1074/jbc.R113.486464>
- 1156 Meade KG, O'Gorman GM, Hill EW, Naciandi F, Agaba M, Kemp SJ, O'Farrelly C, MacHugh DE (2009)
1157 Divergent antimicrobial peptide (AMP) and acute phase protein (APP) responses to *Trypanosoma
1158 congolense* infection in trypanotolerant and trypanosusceptible cattle. *Mol Immunol*, **47**, 196-204.
1159 <https://doi.org/10.1016/j.molimm.2009.09.042>
- 1160 Metcalfe SM (2011) LIF in the regulation of T-cell fate and as a potential therapeutic. *Genes Immun*, **12**,
1161 157-168. <https://doi.org/10.1038/gene.2011.9>
- 1162 Meyer A, Holt HR, Selby R, Guitian J (2016) Past and Ongoing Tsetse and Animal Trypanosomiasis Control
1163 Operations in Five African Countries: A Systematic Review. *PLoS Negl Trop Dis*, **10**, e0005247.
1164 <https://doi.org/10.1371/journal.pntd.0005247>
- 1165 Mills CD, Kincaid K, Alt JM, Heilman MJ, Hill AM (2000) M-1/M-2 macrophages and the Th1/Th2 paradigm.
1166 *J Immunol*, **164**, 6166-6173. <https://doi.org/10.4049/jimmunol.164.12.6166>
- 1167 Mills EL, Kelly B, Logan A, Costa ASH, Varma M, Bryant CE, Tourlomousis P, Dabritz JHM, Gottlieb E, Latorre
1168 I, Corr SC, McManus G, Ryan D, Jacobs HT, Szibor M, Xavier RJ, Braun T, Frezza C, Murphy MP,
1169 O'Neill LA (2016) Succinate Dehydrogenase Supports Metabolic Repurposing of Mitochondria to
1170 Drive Inflammatory Macrophages. *Cell*, **167**, 457-470 e413.
1171 <https://doi.org/10.1016/j.cell.2016.08.064>
- 1172 Mohr E, Cunningham AF, Toellner KM, Bobat S, Coughlan RE, Bird RA, MacLennan IC, Serre K (2010) IFN-
1173 {gamma} produced by CD8 T cells induces T-bet-dependent and -independent class switching in B
1174 cells in responses to alum-precipitated protein vaccine. *Proc Natl Acad Sci USA*, **107**, 17292-17297.
1175 <https://doi.org/10.1073/pnas.1004879107>
- 1176 Morias Y, Abels C, Laoui D, Van Overmeire E, Guilliams M, Schouppe E, Tacke F, DeVries CJ, De Baetselier P,
1177 Beschin A (2015) Ly6C- Monocytes Regulate Parasite-Induced Liver Inflammation by Inducing the
1178 Differentiation of Pathogenic Ly6C+ Monocytes into Macrophages. *PLoS Pathog*, **11**, e1004873.
1179 <https://doi.org/10.1371/journal.ppat.1004873>
- 1180 Morrison LJ, McLellan S, Sweeney L, Chan CN, MacLeod A, Tait A, Turner CM (2010) Role for parasite genetic
1181 diversity in differential host responses to *Trypanosoma brucei* infection. *Infect Immun*, **78**, 1096-
1182 1108. <https://doi.org/10.1128/IAI.00943-09>

- 1183 Morrison LJ, Vezza L, Rowan T, Hope JC (2016) Animal African Trypanosomiasis: Time to Increase Focus on
1184 Clinically Relevant Parasite and Host Species. *Trends Parasitol*, **32**, 599-607.
1185 <https://doi.org/10.1016/j.pt.2016.04.012>
- 1186 Murray M, Trail JC, D'Ieteren GD (1990) Trypanotolerance in cattle and prospects for the control of
1187 trypanosomiasis by selective breeding. *Rev Sci Tech*, **9**, 369-386.
1188 <https://doi.org/10.20506/rst.9.2.506>
- 1189 Murray M, Trail JC, Davis CE, Black SJ (1984) Genetic resistance to African Trypanosomiasis. *J Infect Dis*,
1190 **149**, 311-319. <https://doi.org/10.1093/infdis/149.3.311>
- 1191 Murray PJ (2017) Macrophage Polarization. *Annu Rev Physiol*, **79**, 541-566.
1192 <https://doi.org/10.1146/annurev-physiol-022516-034339>
- 1193 Naessens J (2006) Bovine trypanotolerance: A natural ability to prevent severe anaemia and
1194 haemophagocytic syndrome? *Int J Parasitol*, **36**, 521-528
- 1195 Naessens J, Leak SG, Kennedy DJ, Kemp SJ, Teale AJ (2003) Responses of bovine chimaeras combining
1196 trypanosomosis resistant and susceptible genotypes to experimental infection with *Trypanosoma*
1197 *congolense*. *Vet Parasitol*, **111**, 125-142. [https://doi.org/10.1016/S0304-4017\(02\)00360-6](https://doi.org/10.1016/S0304-4017(02)00360-6)
- 1198 Naessens J, Williams DJ (1992) Characterization and measurement of CD5+ B cells in normal and
1199 *Trypanosoma congolense*-infected cattle. *Eur J Immunol*, **22**, 1713-1718.
1200 <https://doi.org/10.1002/eji.1830220708>
- 1201 Ndoutamia G, Mbakasse RN, Brahim A, Khadidja A (2002) Influence de la Trypanosomose à *T. congolense*
1202 sur les paramètres hématologiques, minéraux et protéo-énergétiques chez les chèvres sahéliennes
1203 du Tchad. *Revue Méd. Vét.*, **153**, 395-400
- 1204 Ned RM, Swat W, Andrews NC (2003) Transferrin receptor 1 is differentially required in lymphocyte
1205 development. *Blood*, **102**, 3711-3718. <https://doi.org/10.1182/blood-2003-04-1086>
- 1206 Noel W, Hassanzadeh G, Raes G, Namangala B, Daems I, Brys L, Brombacher F, Baetselier PD, Beschin A
1207 (2002) Infection stage-dependent modulation of macrophage activation in *Trypanosoma*
1208 *congolense*-resistant and -susceptible mice. *Infect Immun*, **70**, 6180-6187.
1209 <https://doi.org/10.1128/IAI.70.11.6180-6187.2002>
- 1210 Nowyhed HN, Huynh TR, Thomas GD, Blatchley A, Hedrick CC (2015) Cutting Edge: The Orphan Nuclear
1211 Receptor Nr4a1 Regulates CD8+ T Cell Expansion and Effector Function through Direct Repression
1212 of Irf4. *J Immunol*, **195**, 3515-3519. <https://doi.org/10.4049/jimmunol.1403027>
- 1213 Noyes H, Brass A, Obara I, Anderson S, Archibald AL, Bradley DG, Fisher P, Freeman A, Gibson J, Gicheru M,
1214 Hall L, Hanotte O, Hulme H, McKeever D, Murray C, Oh SJ, Tate C, Smith K, Tapió M, Wambugu J,
1215 Williams DJ, Agaba M, Kemp SJ (2011) Genetic and expression analysis of cattle identifies
1216 candidate genes in pathways responding to *Trypanosoma congolense* infection. *Proc Natl Acad Sci
1217 USA*, **108**, 9304-9309. <https://doi.org/10.1073/pnas.1013486108>
- 1218 O'Gorman GM, Park SD, Hill EW, Meade KG, Coussens PM, Agaba M, Naessens J, Kemp SJ, MacHugh DE
1219 (2009) Transcriptional profiling of cattle infected with *Trypanosoma congolense* highlights gene
1220 expression signatures underlying trypanotolerance and trypanosusceptibility. *BMC Genomics*, **10**,
1221 207. <https://doi.org/10.1186/1471-2164-10-207>
- 1222 O'Gorman GM, Park SD, Hill EW, Meade KG, Mitchell LC, Agaba M, Gibson JP, Hanotte O, Naessens J, Kemp
1223 SJ, MacHugh DE (2006) Cytokine mRNA profiling of peripheral blood mononuclear cells from
1224 trypanotolerant and trypanosusceptible cattle infected with *Trypanosoma congolense*. *Physiol
1225 Genomics*, **28**, 53-61. <https://doi.org/10.1152/physiolgenomics.00100.2006>
- 1226 O'Neill LA, Kishton RJ, Rathmell J (2016) A guide to immunometabolism for immunologists. *Nat Rev
1227 Immunol*, **16**, 553-565. <https://doi.org/10.1038/nri.2016.70>
- 1228 O'Rawe JA, Ferson S, Lyon GJ (2015) Accounting for uncertainty in DNA sequencing data. *Trends Genet*, **31**,
1229 61-66. <https://doi.org/10.1016/j.tig.2014.12.002>
- 1230 Obermajer N, Repnik U, Jevnikar Z, Turk B, Kreft M, Kos J (2008) Cysteine protease cathepsin X modulates
1231 immune response via activation of beta2 integrins. *Immunology*, **124**, 76-88.
1232 <https://doi.org/10.1111/j.1365-2567.2007.02740.x>
- 1233 Okwor I, Onyilagha C, Kuriakose S, Mou Z, Jia P, Uzonna JE (2012) Regulatory T cells enhance susceptibility
1234 to experimental *Trypanosoma congolense* infection independent of mouse genetic background.
1235 *PLoS Negl Trop Dis*, **6**, e1761. <https://doi.org/10.1371/journal.pntd.0001761>

- 1236 Onyilagha C, Jia P, Jayachandran N, Hou S, Okwor I, Kuriakose S, Marshall A, Uzonna JE (2015) The B cell
1237 adaptor molecule Bam32 is critically important for optimal antibody response and resistance to
1238 *Trypanosoma congolense* infection in mice. *PLoS Negl Trop Dis*, **9**, e0003716.
1239 <https://doi.org/10.1371/journal.pntd.0003716>
- 1240 Onyilagha C, Kuriakose S, Ikeogu N, Jia P, Uzonna J (2018) Myeloid-Derived Suppressor Cells Contribute to
1241 Susceptibility to *Trypanosoma congolense* Infection by Suppressing CD4(+) T Cell Proliferation and
1242 IFN-gamma Production. *J Immunol*, **201**, 507-515. <https://doi.org/10.4049/jimmunol.1800180>
- 1243 Paillard F, Sterkers G, Vaquero C (1990) Transcriptional and post-transcriptional regulation of TcR, CD4 and
1244 CD8 gene expression during activation of normal human T lymphocytes. *EMBO J*, **9**, 1867-1872.
1245 <https://doi.org/10.1002/j.1460-2075.1990.tb08312.x>
- 1246 Payne WJA, Hodges J (1997) *Tropical cattle, origins, breeds and breeding policies*. Blackwell Science, Oxford.
- 1247 Pearce EL, Pearce EJ (2013) Metabolic pathways in immune cell activation and quiescence. *Immunity*, **38**,
1248 633-643. <https://doi.org/10.1016/j.jimmuni.2013.04.005>
- 1249 Pello OM, De Pizzol M, Mirolo M, Soucek L, Zammataro L, Amabile A, Doni A, Nebuloni M, Swigart LB, Evan
1250 GI, Mantovani A, Locati M (2012) Role of c-MYC in alternative activation of human macrophages
1251 and tumor-associated macrophage biology. *Blood*, **119**, 411-421. <https://doi.org/10.1182/blood-2011-02-339911>
- 1252 Pierre C (1906) *L'élevage en Afrique occidentale française*. Gouvernement général de l'Afrique occidentale
1253 française, Inspection de l'agriculture, Paris.
- 1254 Pinder M, Bauer J, Van Melick A, Fumoux F (1988) Immune responses of trypanoresistant and
1255 trypanosusceptible cattle after cyclic infection with *Trypanosoma congolense*. *Vet Immunol
1256 Immunopathol*, **18**, 245-257. [https://doi.org/10.1016/0165-2427\(88\)90069-4](https://doi.org/10.1016/0165-2427(88)90069-4)
- 1257 Rajavel A, Heinrich F, Schmitt AO, Gultas M (2020) Identifying Cattle Breed-Specific Partner Choice of
1258 Transcription Factors during the African Trypanosomiasis Disease Progression Using Bioinformatics
1259 Analysis. *Vaccines (Basel)*, **8**. <https://doi.org/10.3390/vaccines8020246>
- 1260 Team RC (2018) R: A language and environment for statistical computing. R Foundation for Statistical
1261 Computing, Vienna, Austria. URL <http://www.R-project.org/>.
- 1262 Rege JE (1999) The state of African cattle genetic resources I. Classification framework and identification
1263 of threatened and extinct breeds. *AGRI*, **25**, 1-25
- 1264 Risco A, del Fresno C, Mambol A, Alsina-Beauchamp D, MacKenzie KF, Yang HT, Barber DF, Morcelle C,
1265 Arthur JS, Ley SC, Ardevin C, Cuenda A (2012) p38gamma and p38delta kinases regulate the Toll-
1266 like receptor 4 (TLR4)-induced cytokine production by controlling ERK1/2 protein kinase pathway
1267 activation. *Proc Natl Acad Sci U S A*, **109**, 11200-11205. <https://doi.org/10.1073/pnas.1207290109>
- 1268 Ritchie ME, Phipson B, Wu D, Hu Y, Law CW, Shi W, Smyth GK (2015) limma powers differential expression
1269 analyses for RNA-sequencing and microarray studies. *Nucleic Acids Res*, **43**, e47.
1270 <https://doi.org/10.1093/nar/gkv007>
- 1271 Roberts CJ, Gray AR (1973) Studies on trypanosome-resistant cattle. II. The effect of trypanosomiasis on
1272 N'dama, Muturu and Zebu cattle. *Trop Anim Health Prod*, **5**, 220-233.
1273 <https://doi.org/10.1007/BF02240423>
- 1274 Robinson MD, McCarthy DJ, Smyth GK (2010) edgeR: a Bioconductor package for differential expression
1275 analysis of digital gene expression data. *Bioinformatics*, **26**, 139-140.
1276 <https://doi.org/10.1093/bioinformatics/btp616>
- 1277 Schulman IG (2017) Liver X receptors link lipid metabolism and inflammation. *FEBS Lett*, **591**, 2978-2991.
1278 <https://doi.org/10.1002/1873-3468.12702>
- 1279 Seck MT, Bouyer J, Sall B, Bengaly Z, Vreyen MJ (2010) The prevalence of African animal trypanosomoses
1280 and tsetse presence in Western Senegal. *Parasite*, **17**, 257-265.
1281 <https://doi.org/10.1051/parasite/2010173257>
- 1282 Sileghem M, Flynn JN (1992a) Suppression of interleukin 2 secretion and interleukin 2 receptor expression
1283 during tsetse-transmitted trypanosomiasis in cattle. *Eur J Immunol*, **22**, 767-773.
1284 <https://doi.org/10.1002/eji.1830220321>
- 1285 Sileghem M, Flynn JN (1992b) Suppression of T-cell responsiveness during tsetse-transmitted
1286 trypanosomiasis in cattle. *Scand J Immunol Suppl*, **11**, 37-40. <https://doi.org/10.1111/j.1365-3083.1992.tb01616.x>

- 1289 Sileghem MR, Flynn JN, Saya R, Williams DJ (1993) Secretion of co-stimulatory cytokines by monocytes and
1290 macrophages during infection with *Trypanosoma (Nannomonas) congolense* in susceptible and
1291 tolerant cattle. *Vet Immunol Immunopathol*, **37**, 123-134. [https://doi.org/10.1016/0165-2427\(93\)90060-H](https://doi.org/10.1016/0165-2427(93)90060-H)
- 1293 Swallow BM (2000) *Impacts of Trypanosomiasis on African agriculture*. PAAT Technical and scientific series
1294 2. FAO (Food and Agricultural Organization of the United Nations), Rome, Italy.
- 1295 Taiwo VO, Anosa VO (2000) *In vitro* erythrophagocytosis by cultured macrophages stimulated with
1296 extraneous substances and those isolated from the blood, spleen and bone marrow of Boran and
1297 N'Dama cattle infected with *Trypanosoma congolense* and *Trypanosoma vivax*. *Onderstepoort Journal of Veterinary Research*, **67**, 273-287
- 1299 Taylor KA (1998) Immune responses of cattle to African trypanosomes: protective or pathogenic? *Int J Parasitol*, **28**, 219-240. [https://doi.org/10.1016/S0020-7519\(97\)00154-9](https://doi.org/10.1016/S0020-7519(97)00154-9)
- 1301 Taylor KA, Lutje V, Kennedy D, Authie E, Boulange A, Logan-Henfrey L, Gichuki B, Gettinby G (1996)
1302 *Trypanosoma congolense*: B-lymphocyte responses differ between trypanotolerant and
1303 trypanosusceptible cattle. *Exp Parasitol*, **83**, 106-116. <https://doi.org/10.1006/expr.1996.0054>
- 1304 Taylor KA, Mertens B (1999) Immune response of cattle infected with African trypanosomes. *Mem Inst Oswaldo Cruz*, **94**, 239-244
- 1306 Trail JC, d'Ieteren GD, Maille JC, Yangari G (1991) Genetic aspects of control of anaemia development in
1307 trypanotolerant N'Dama cattle. *Acta Trop*, **48**, 285-291. [https://doi.org/10.1016/0001-706X\(91\)90016-D](https://doi.org/10.1016/0001-706X(91)90016-D)
- 1309 Trail JC, Wissocq N, d'Ieteren GD, Kakiese O, Murray M (1994) Quantitative phenotyping of N'Dama cattle
1310 for aspects of trypanotolerance under field tsetse challenge. *Vet Parasitol*, **55**, 185-195.
1311 [https://doi.org/10.1016/0304-4017\(94\)00649-W](https://doi.org/10.1016/0304-4017(94)00649-W)
- 1312 Traore-Leroux T, Fumoux F, Pinder M (1987) High density lipoprotein levels in the serum of
1313 trypanosensitive and trypanoresistant cattle. Changes during *Trypanosoma congolense* infection.
1314 *Acta Trop*, **44**, 315-323
- 1315 Uilenberg G (1998) A field guide for the diagnosis, treatment and prevention of African animal
1316 trypanosmosis. FAO, Rome.
- 1317 Uzonna JE, Kaushik RS, Zhang Y, Gordon JR, Tabel H (1998) Experimental murine *Trypanosoma congolense*
1318 infections. II. Role of splenic adherent CD3+Thy1.2+ TCR-alpha beta- gamma delta- CD4+8- and
1319 CD3+Thy1.2+ TCR-alpha beta- gamma delta- CD4-8- cells in the production of IL-4, IL-10, and IFN-
1320 gamma and in trypanosome-elicited immunosuppression. *J Immunol*, **161**, 6189-6197
- 1321 Van de Laar L, Coffer PJ, Wolftman AM (2012) Regulation of dendritic cell development by GM-CSF:
1322 molecular control and implications for immune homeostasis and therapy. *Blood*, **119**, 3383-3393.
1323 <https://doi.org/10.1182/blood-2011-11-370130>
- 1324 Van der Waaij EH, Hanotte O, Van Arendonk JAM, Kemp SJ, Kennedy D, Gibson A, Teale A (2003) Population
1325 parameters for traits defining trypanotolerance in a F2 cross of N'Dama and Boran cattle. *Livest Sci*, **84**, 219-230. [https://doi.org/10.1016/S0301-6226\(03\)00078-2](https://doi.org/10.1016/S0301-6226(03)00078-2)
- 1327 Vincendeau P, Bouteille B (2006) Immunology and immunopathology of African trypanosomiasis. *An Acad Bras Cienc*, **78**, 645-665. <https://doi.org/10.1590/S0001-37652006000400004>
- 1329 Vulcano M, Albanesi C, Stoppacciaro A, Bagnati R, D'Amico G, Struyf S, Transidico P, Bonecchi R, Del Prete
1330 A, Allavena P, Ruco LP, Chiabrando C, Girolomoni G, Mantovani A, Sozzani S (2001) Dendritic cells
1331 as a major source of macrophage-derived chemokine/CCL22 in vitro and in vivo. *Eur J Immunol*,
1332 **31**, 812-822. [https://doi.org/10.1002/1521-4141\(200103\)31:3<812::AID-IMMU812>3.0.CO;2-L](https://doi.org/10.1002/1521-4141(200103)31:3<812::AID-IMMU812>3.0.CO;2-L)
- 1334 Wang LM, Zhang Y, Li X, Zhang ML, Zhu L, Zhang GX, Xu YM (2018) Nr4a1 plays a crucial modulatory role in
1335 Th1/Th17 cell responses and CNS autoimmunity. *Brain Behav Immun*, **68**, 44-55.
1336 <https://doi.org/10.1016/j.bbi.2017.09.015>
- 1337 Wang R, Dillon CP, Shi LZ, Milasta S, Carter R, Finkelstein D, McCormick LL, Fitzgerald P, Chi H, Munger J,
1338 Green DR (2011) The transcription factor Myc controls metabolic reprogramming upon T
1339 lymphocyte activation. *Immunity*, **35**, 871-882. <https://doi.org/10.1016/j.jimmuni.2011.09.021>
- 1340 Whitehead A, Crawford DL (2006) Neutral and adaptive variation in gene expression. *Proc Natl Acad Sci U
1341 S A*, **103**, 5425-5430. <https://doi.org/10.1073/pnas.0507648103>

- 1342 Wickham H (2016) *ggplot2: Elegant graphics for data analysis*. Springer International Publishing, New York.
- 1343 Wilson KC, Center DM, Cruikshank WW (2004) The effect of interleukin-16 and its precursor on T
1344 lymphocyte activation and growth. *Growth Factors*, **22**, 97-104.
1345 <https://doi.org/10.1080/08977190410001704679>
- 1346 Xu J, Flaczyk A, Neal LM, Fa Z, Eastman AJ, Malachowski AN, Cheng D, Moore BB, Curtis JL, Osterholzer JJ,
1347 Olszewski MA (2017) Scavenger Receptor MARCO Orchestrates Early Defenses and Contributes to
1348 Fungal Containment during Cryptococcal Infection. *J Immunol*, **198**, 3548-3557.
1349 <https://doi.org/10.4049/jimmunol.1700057>
- 1350 Yoon MS (2017) The Role of Mammalian Target of Rapamycin (mTOR) in Insulin Signaling. *Nutrients*, **9**.
1351 <https://doi.org/10.3390/nu9111176>
- 1352 Zamboni DS, Lima-Junior DS (2015) Inflammasomes in host response to protozoan parasites. *Immunol Rev*,
1353 **265**, 156-171. <https://doi.org/10.1111/imr.12291>
- 1354 Zoldan K, Moellmer T, Schneider J, Fueldner C, Knauer J, Lehmann J (2014) Increase of CD25 expression on
1355 bovine neutrophils correlates with disease severity in post-partum and early lactating dairy cows.
1356 *Dev Comp Immunol*, **47**, 254-263. <https://doi.org/10.1016/j.dci.2014.08.002>

1357